40th Annual Ohio River Valley Soils Seminar
ORVSS XL

GEOTECHNICAL ENGINEERING AND ENERGY INFRASTRUCTURE

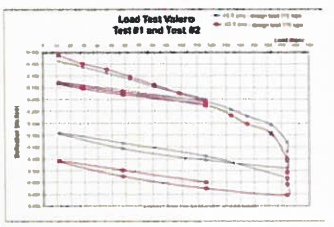

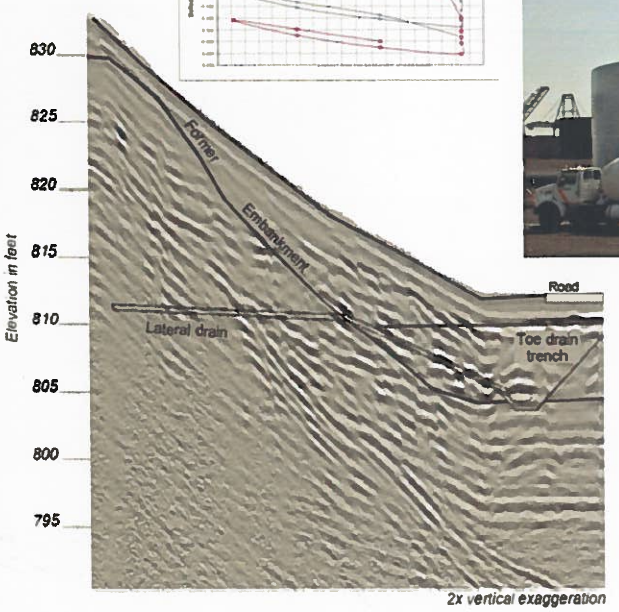

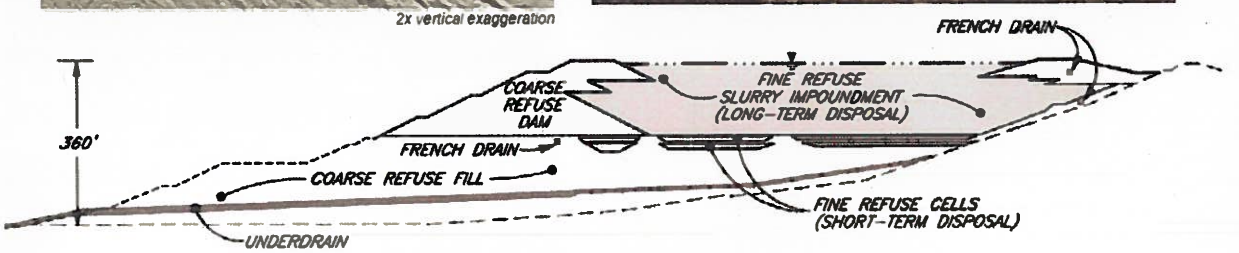

November 13, 2009
Lexington Convention Center
Lexington, Kentucky

ORVSS XL
SEMINAR AGENDA

7:30-8:10 Registration

MORNING SESSION

8:10-8:15 Opening Remarks (Michael Kalinski, University of Kentucky)

8:15-9:00 Gary Brill, Geo/Environmental Associates, **"Innovative Design and Construction of Coal Refuse Disposal Facilities--Two Case Histories"**

9:00-9:15 Break

9:15-10:00 Mutiu G. Ayoola and Vincent O. Ogunro, University of North Carolina, Charlotte, **"Geotechnical Aspects of Nuclear Power Plant Design: A Review"**

10:00-10:15 Break

10:15-11:00 R. J. Franz and A. L. Sehn, Hayward Baker, Inc., **"Ethanol Plant Supported on Aggregate Pier Foundation System"**

11:00-11:15 Break

11:15-12:00 Scott Ludlow, Earth Exploration, Inc., **"Evaluation of Voids within an Earth Embankment"**

12:00-1:00 Lunch

AFTERNOON SESSION

1:00-1:45 KEYNOTE SPEAKER: Kenneth H. Stokoe II, University of Texas at Austin, **"Field Seismic Investigations at Sites Proposed for Nuclear Plants and High-Level Radioactive Waste Facilities"**

1:45-2:00 Break

2:00-2:45 Frederic Masse, Seth L. Pearlman, and Martin G. Taube, DGI-Menard, Inc., **"Controlled Modulus Columns™ (CMC) for Support of Above-Ground Storage Tanks"**

2:45-3:00 Break

3:00-3:45 Barry F. Beck, Arthur Pettit, and Wanfang Zhou, P.E. LaMoreaux & Associates, **"Evaluation of Karstic Foundation Hazards for New Power Plant Construction at a Site in Central Florida"**

3:45-4:00 Closing Remarks (Michael Kalinski, University of Kentucky)

PROCEEDINGS OF THE FORTIETH

OHIO RIVER VALLEY SOILS SEMINAR

GEOTECHNICAL ENGINEERING and ENERGY INFASTRUCTURE

November 13, 2009

Lexington Convention Center

Lexington, Kentucky

Sponsored by

Kentucky Geotechnical Engineering Group, ASCE

University of Kentucky
Department of Civil Engineering

And

University of Louisville
Department of Civil and Environmental Engineering

University Of Cincinnati
Department of Civil and Environmental Engineering

Cincinnati Geotechnical Group, ASCE

ORVSS XL
ORGANIZING COMMITTEE

Malcolm Barrett, PE
ATC Associates, Inc.

Michael E. Kalinski, PE
University of Kentucky

Timothy C. Barnett Jr., PE
Stantec

Charles S. Bishop, PE
Bowser Morner Associates, Inc.

Joe Cooke, PE
CSI of Kentucky

TABLE OF CONTENTS

Innovative Design and Construction of Coal Refuse Disposal Facilities – Two Case Histories

Gary T. Brill, P.E.
Vice President
Geo/Environmental Associates, Inc.
3502 Overlook Circle
Knoxville, Tennessee 37909
Tel: 865-584-0344
Fax: 865-584-0778
Email: gbrill@geoe.com

ABSTRACT. As a result of increased environmental and political scrutiny of the coal mining industry, the use of innovative and cost efficient designs for bulk waste handling from coal processing operations has become critical for our nation's largest energy source. Construction of coal tailings impoundments remains an efficient and safe method of waste disposal. This paper will present two contrasting case histories of coal refuse impoundments.

Case History No. 1 details the design, construction and operation of a Slurry Impoundment facility that was carefully studied for efficient dam construction, fine refuse disposal volumes, and maximum coal recovery. Unique design features include constructing a 300 feet high, nearly two million cubic yard embankment dam almost entirely of segregated contour mine overburden materials, and using up to 10 feet thick lifts of bulk sandstone rockfill in portions of the dam. A few years after completion of the dam, plant capacity and coal reserves were increased, necessitating raising the dam height an additional 100 feet using coarse refuse fill and the upstream construction method.

In contrast to the site of the first case history, the site of Case History No. 2 was never intended to be a slurry impoundment. An established preparation plant disposed of its coal refuse with a combination of injecting fine refuse into underground abandoned mine workings and constructing a coarse refuse embankment fill. After underground injection disposal capacity was unexpectedly depleted, the plant was idled until short-term fine refuse cells could be designed and constructed on the surface of the coarse refuse embankment. The cells were then converted to a slurry impoundment for long-term refuse disposal. Mitigative measures were required to deal with difficult pre-existing geologic and abandoned underground mine-related conditions.

KEYWORDS. Coal refuse, slurry impoundments, deep mine workings, upstream construction, drained hillside embankments.

INTRODUCTION

The most common methods to recover coal from the earth are surface mining and deep mining. Surface mining involves the removal and replacement of hillside rock above the coal so that the coal can be removed efficiently by conventional earth-moving equipment. Surface mining can be limited to a segment running parallel to the hillside (contour mining) or extended to a large area (mountain top removal). Deep mining involves the removal of coal from beneath the intact ground surface by creating a series of structural tunnels, or mines, into the hard rock layer overlying the coal. Typically, the raw coal material removed from the deep mine is comprised of about 50% coal and about 50% shale, sand, silt and clay.

Coal preparation plants are necessary to remove the coal from the non-coal (refuse) material, and the result is large volumes of refuse that require proper disposal. The coal refuse is often split into a coarse refuse (mostly shale rock) and fine refuse (sand, silt and clay size particles). An efficient method of disposal in the Appalachian coalfields is to create a structural embankment dam across a hollow using the coarse refuse and pump the fine refuse in a slurry to fill behind the dam. Coal refuse slurry impoundments normally have an operating life that matches the preparation plant and coal reserves, often in excess of 20 years.

To best utilize the resources of an undisturbed hollow, contour surface mining and slurry impoundment design can be combined as will be described in Case History No. 1. A significant challenge for the coal industry is the existence of fewer undisturbed hollows over time as coal resources are removed by both surface and deep mining. Case History No. 2 explores the challenges involved with using an available disturbed hollow for constructing a slurry impoundment under less than ideal conditions.

CASE HISTORY NO. 1

Planning and Site Selection

Site selection consisted of examining four undisturbed hollows surrounding the plant site. The hollows were rated considering:

- Recoverable Coal (Two coal seams were identified for surface mining)
- Dam considerations including a narrow hollow for efficient dam construction, available borrow material to build the dam, a small contributing watershed, and the ability to raise the dam in the future
- Environmental concerns and downstream conditions

Most coal refuse slurry impoundments are constructed using the coarse refuse material to build a continuously raised embankment dam. The unique feature that was included in the planning phase was to construct a nearly 2 million cubic yard dam almost entirely of contour mine overburden materials in a relatively short period of time. Exploratory drilling was performed to characterize the overburden materials and estimate the relative volumes of sandstone, shale and soil materials as well as examine the subsurface for dam construction.

Design and Regulatory Review

A slurry impoundment design was developed that included segregating the mine overburden materials into distinct embankment zones. As shown on Figure 1, the zones included a clay earthfill zone with core trench cutoff in rock, a random soil zone (mostly silt, sand and gravel sized particles), a weathered shale rockfill zone, and a bulk sandstone rockfill zone. For efficient construction, the sandstone rockfill was proposed to be constructed in 10 feet thick lifts and the more weatherable shale rockfill in 3 feet thick lifts.

Slurry impoundment designs must be reviewed and approved by both Federal (Mine Safety and Health Administration, or MSHA) and state agencies. Regulatory concerns for the project included the potential for excessive settlement and deformation of the thick lift rockfill zones and piping of soil materials between the embankment zones. These concerns were addressed by incorporating a settlement monitoring plan for during and after construction, the design of a filter zone between the large sandstone rockfill zone and the remainder of the embankment dam, and by performing large scale grain-size estimations of the blasted mine overburden materials to verify compliance with filter criteria.

Construction

The keys to successful construction were making accurate estimates of the various available embankment materials and then having a knowledgeable site manager (or "traffic cop") to direct trucks to the appropriate embankment zone (refer to Figure 2). Further, a screening plant was established to generate rockfill for the embankment filter zone. Post-construction settlements listed in Table 1 were within tolerable limits.

TABLE 1
Post-Construction Settlement Along Dam Profile

DAM HEIGHT (FT)	SETTLEMENT (FT)	% STRAIN
230	2.4	1.0
200	2.2	1.1
180	1.9	1.1
150	1.3	0.9
135	1.7	1.2
105	1.2	1.1
75	0.9	1.2
30	0.6	2.0

After finishing construction of the dam, fine refuse disposal consisted of filling behind the dam and maintaining a "beach" of material on the upstream embankment face for added seepage control. Within a few years the decision was made to enlarge the plant and increase production. This necessitated raising the embankment dam an additional 100 feet using coarse refuse and the upstream construction method (i.e., constructing the embankment over top of the beach of fine refuse tailings) as shown in Figures 3 and 4. The key to successful upstream construction includes starting the construction as early as

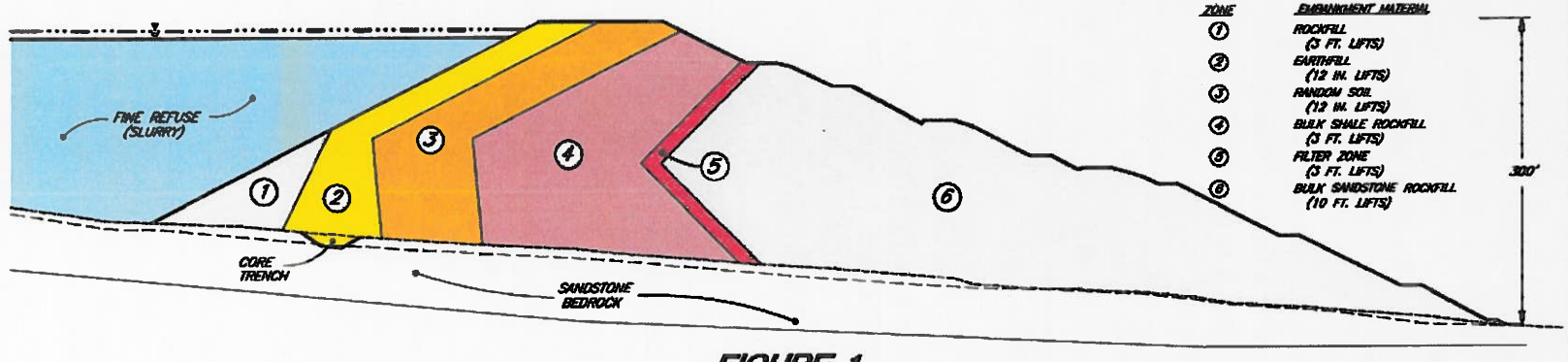

FIGURE 1

CASE HISTORY NO. 1 DAM DESIGN PROFILE

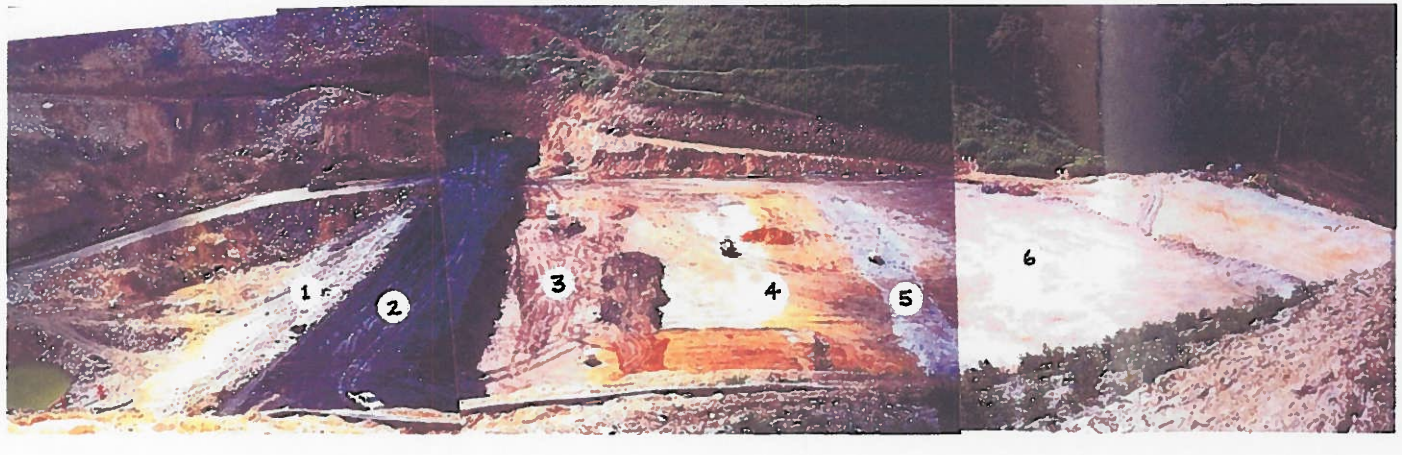

FIGURE 2

CASE HISTORY NO. 1 DAM CONSTRUCTION PROFILE

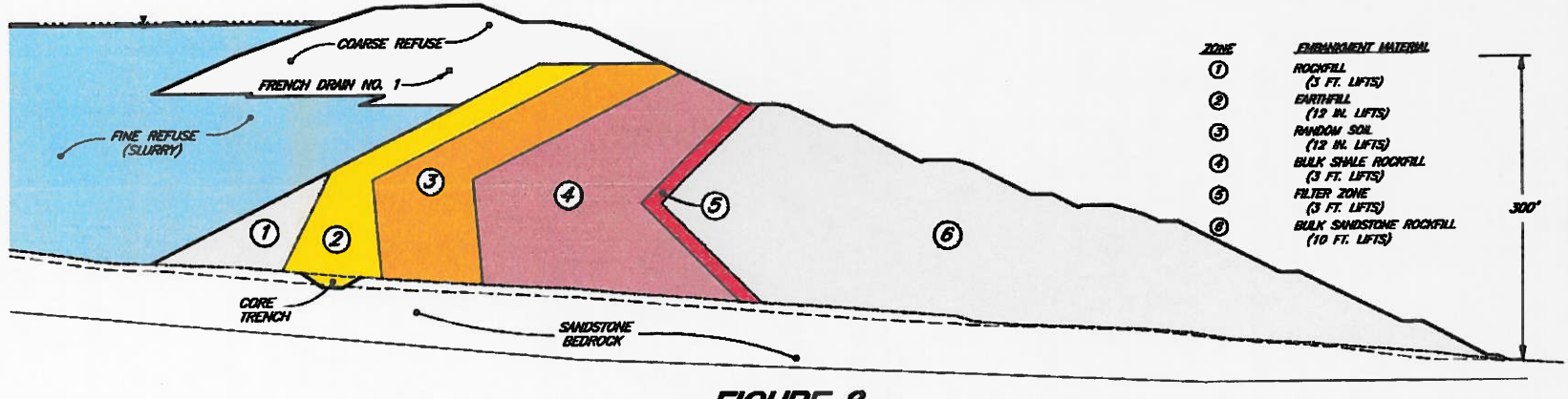

FIGURE 3

CASE HISTORY NO. 1 ENLARGED DAM PROFILE

FIGURE 4

CASE HISTORY NO. 1 FINAL DAM WITH UPSTREAM STAGE

possible (before the pond is full) so that a narrow embankment hinge just upstream of the dam is avoided. Further, additional internal drains in the raised embankment and monitoring of pore pressures beneath the embankment pushout over the fines were incorporated into the design.

CASE HISTORY NO. 2

Background

The preparation plant for Case History No. 2 operated by injecting fine refuse into abandoned underground mine workings and constructing a coarse refuse pile. When the injection hole for fines plugged unexpectedly, the plant was idled. Short-term fine refuse cells constructed on the surface of the coarse refuse pile were quickly designed and approved while plans for long-term disposal were developed. Each cell was less than 20 feet deep and 20 acre-feet in capacity. A total of 8 cells were used to keep the plant running for 1.5 years. Figure 5 shows excavated cells ready for pumping fines. Long term disposal consisted of converting the coarse refuse pile to a slurry impoundment.

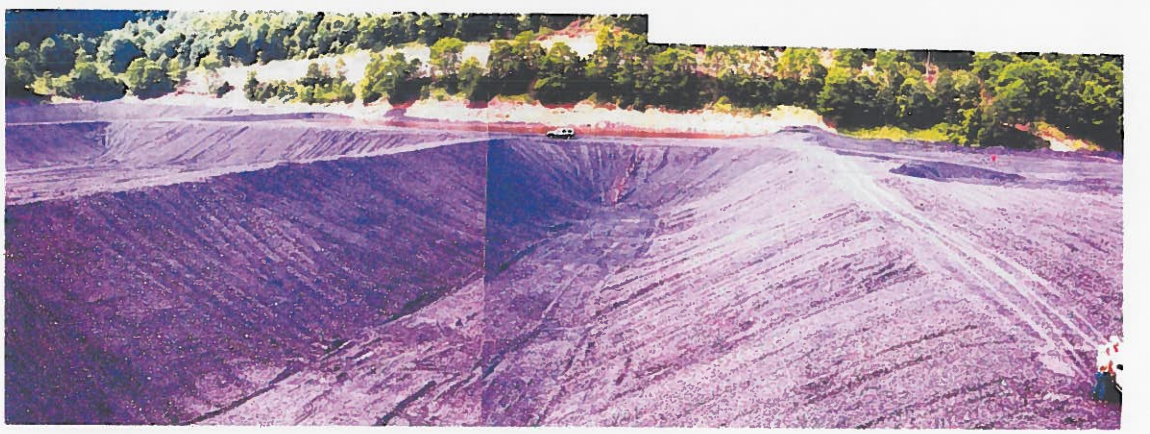

FIGURE 5
CASE HISTORY NO. 2
EXCAVATED FINE REFUSE CELLS

Design

The conversion to a slurry impoundment was viable because of the large surface area on the crest of the coarse refuse pile and the small contributing watershed area (i.e., less than 50 acres). There were several difficulties for the conversion including previous surface mining, auger mining, deep mining and the resulting fractured hillside rock at the site. As a conservative measure, and to expedite regulatory approvals, a drained hillside embankment was proposed to extend around the entire pond perimeter. The intent of the embankment was to separate the fine refuse pond from the natural hillsides. Further, the hillsides were to be stripped to rock to expose any undesirable hillside features. These design measures had successfully been used at two sites in Virginia after breakthroughs of fine refuse into abandoned mine workings had occurred. In addition, seismic cross-hole work was performed to verify mine mapping, and instrumentation was installed at key

locations in the hillsides to monitor for potential mine subsidence and for water levels in the mine workings and original highwall backfill materials. An illustration of the difficult hillside conditions is included as Figure 6.

Construction

The conversion to an impoundment was made using coarse refuse to build a raised main embankment dam and eventually a smaller saddle embankment as shown in Figures 7 and 8. The converted facility has successfully operated for over 11 years of a proposed total 15 year design life. The final constructed height of the facility will be 360 feet.

LESSONS LEARNED

Experience learned from the two case histories includes:

1. Think long-term when designing refuse disposal facilities
2. Be adaptable and have options if the life of the coal reserves changes
3. Innovate using sound engineering judgement
4. Make regulatory reviewers partners in the design process by getting their input and buy-in early in the project especially when innovating

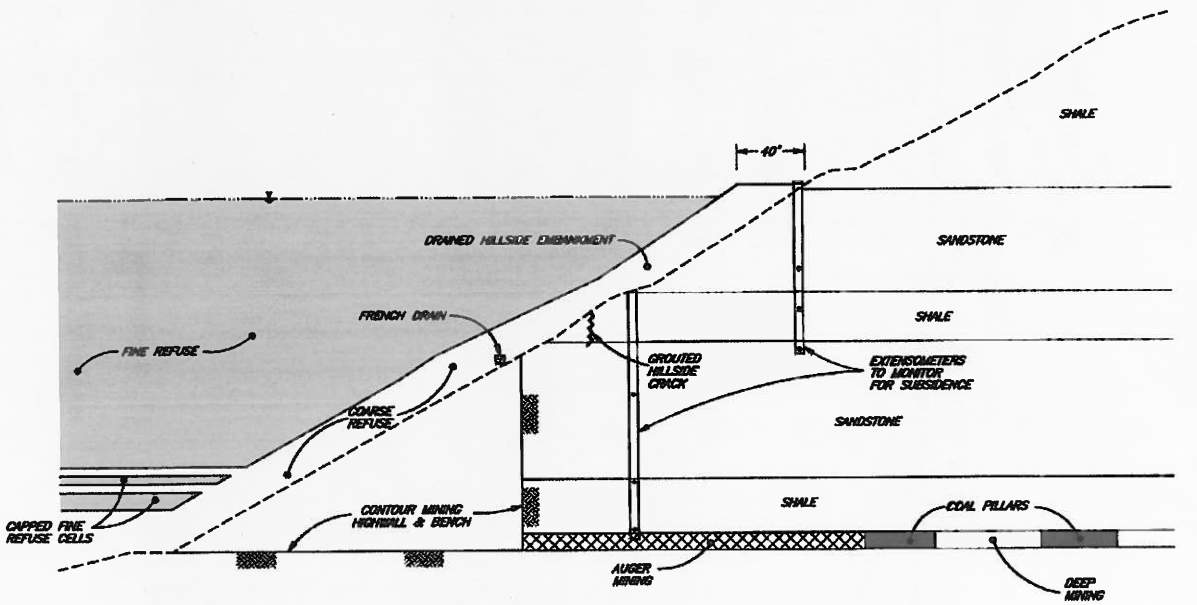

FIGURE 6

CASE HISTORY NO. 2 HILLSIDE SECTION

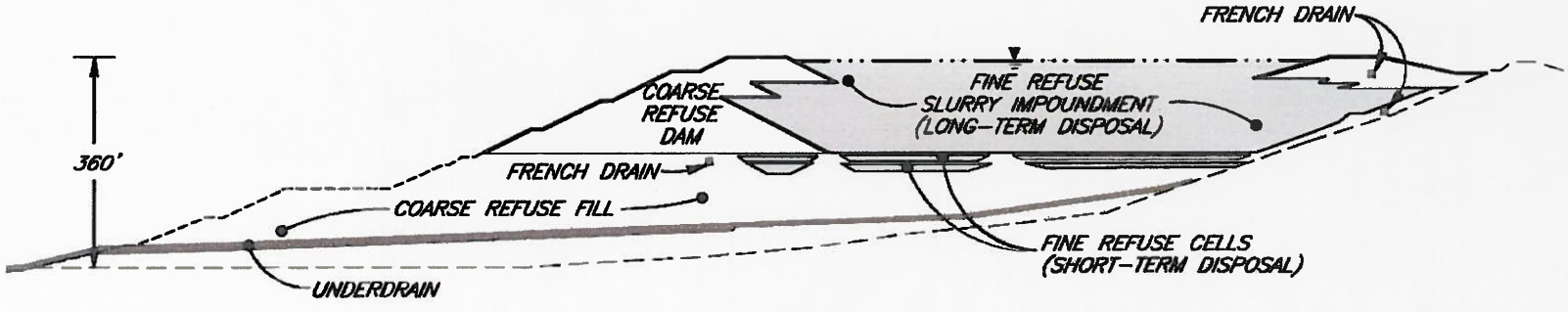

FIGURE 7

CASE HISTORY NO. 2 DAM PROFILE

FIGURE 8

CASE HISTORY NO. 2
SLURRY IMPOUNDMENT WITH HILLSIDE EMBANKMENT

Geotechnical Aspects of Nuclear Power Plants Design: A Review

Mutiu G. Ayoola, Ph.D., P.E[1] and Vincent O. Ogunro, Ph.D[2]

Increasing number of nuclear power plants (NPPs) are currently under design across the globe. In Europe and Asia, more than thirty (30) new NPP units have been approved by regulatory agencies and some are already under construction. However, considering that no new NPP have been designed or constructed in the last few decades; the analysis, design, and construction of these new generation of plants to meet the revised and more conservative safety regulatory requirements are quite challenging.

The new generation NPPs are extremely heavy infrastructures due to additional structural safety requirements following the 9/11 terrorist attack and the 1996 Chernobyl accident. The new NPP foundation may impose bearing pressures of more than 50 ksf on the supporting soil. For safety purposes, the plants are required to be designed for very conservative earthquake motion and geotechnical criteria. For example, in the event of no site specific studies, it is not uncommon for the plants to be designed for earthquake-induced ground acceleration of 0.45g; limited differential settlement of less than 2 inches to avoid failure of buried pipes; minimum shear wave velocity of 1000 ft/s for the backfill material to provide stability against liquefaction; minimum factor of safety of 1.4 against sliding and overturning under static and dynamic loading conditions.

In order to achieve some of the geotechnical criteria that are required of the new NPPs, innovative analysis and design concepts are continuously being developed and utilized. This paper provides an overview of some of the geotechnical challenges and lessons learned during the analysis and design of some of these plants. For example, the need to depend on the passive soil condition where the resistance provided by the foundation base friction is not adequate to provide stability against sliding. In most cases, due to regulatory requirements, the maximum passive soil pressure is not mobilized. This necessitates the need for a soil deformation-based passive soil pressure in the design of the embedded structural walls

Keyword: Nuclear Plant, Liquefaction, Settlement, Sliding, Seismic, Stability

1: Formerly doctoral student, Department of Civil Engineering, University of North Carolina, Charlotte. E-mail: mgbolagade@yahoo.com. Tel.: 704 576 3776.

2: Associate Professor, Department of Civil Engineering, University of North Carolina, Charlotte. E-mail: vogunro@uncc.edu. Tel. 704 687 3101

Introduction

Nuclear power plants generate more than 20% of energy consumed in the US. Aside from concern related to management of the spent fuel, nuclear power plants are considered environmental friendly as they do not release CO_2 or other greenhouse gases into the environment. However, after the 1996 Chernobyl incident, the nuclear industry suffered tremendous set back. The nuclear industry is currently experiencing a resurgence of interest due to increasing global demand for energy. According to the U.S. Nuclear Regulatory Commission (NRC) which is responsible for licensing of engineering design and construction of new nuclear power plants and radioactive waste containment facilities, more than twenty (20) license applications have been submitted by utility plants companies that intend to design, construct, and operate new nuclear plants.

The analysis and design requirements of new nuclear plants are more conservative following the 9/11 attack and the 1996 Chernobyl nuclear accident. Significant structural components of new designs are buried below grade level to minimize susceptibility to terrorist attack and the potential for release of radioactive materials into the environment. NRC requires that the civil and mechanical structures be designed to resist very conservative earthquake motion. In the absence of site specific seismological data, some of the new NPP are analyzed and designed to withstand earthquake-induced ground acceleration of more than 0.3g for the plant to safely shutdown without any major structural damage. This ground acceleration value which is referred to as the safe shutdown earthquake (SSE) is very conservative. New NPP are extremely heavy infrastructures and foundation dynamic bearing pressure of more than 50 ksf has been reported especially under earthquake-induced dynamic loads. Depending on the relative stiffness of the nuclear plant structure and the foundation soil, the earthquake motion and the structural response may be amplified or dampened. For very stiff structures founded on loose soil, the presence of the structure will typically reduce the response while a structure of low stiffness compared with the foundation soil will amplify the ground motion and structure response. A detailed soil-structure interaction analysis is required to establish how the presence of the structure influences the natural response of the soil deposits.

Most new nuclear power plants will experience foundation sliding under design earthquake motion. To eliminate structural and piping failures, NRC limits the maximum foundation sliding to an acceptable value that will not cause structural distress. In some cases,

reinforced concrete walls embedded below grade are relied upon to provide some resistance. This is achieved by considering static and dynamic passive soil pressures in the design of the embedded walls. Loose and saturated granular soils under earthquake load will experience liquefaction. To avoid liquefaction and loss of support, foundation is founded on rock or competent soil that is not susceptible to liquefaction. For regulatory purpose, a competent soil is referred to as soil having a minimum shear wave velocity of 1000 ft/s.

Nuclear plant sites typically include several buildings such as the containment building where the nuclear reaction process takes place; the emergency power generating building which provides temporary power when the nuclear plants shut down for any other reason besides maintenance; and other auxiliary buildings. Some of the buildings are rigidly connected and supported by a common mat foundation while others are supported by separate mat foundation.

Typically, the containment building is heavier than other structures and will impose higher magnitude of foundation bearing pressure. Therefore, settlement under the containment building is generally higher. Buried pipes connected rigidly to the containment and adjacent buildings may experience failure if the buildings differential settlement is excessive.

Some geotechnical challenges and concepts developed to address issues related to buildings differential settlements; liquefaction, bearing capacity, and foundation sliding failures; and soil structure interaction effects; are discussed. Due to security concerns and regulatory requirements, actual data, analyses, and designs related to NPP are considered as safeguard information, classified, and not available to the public. Therefore, the intent of this paper is not to present data related to analysis, design, and construction of a NPPP. Rather, general overview of the geotechnical problems associated with the analysis and design of new NPP are presented.

Foundation Stability

A mat foundation is mostly used to support nuclear plant structures. Pile foundations are rarely used. A mat foundation offered the advantage of stress redistribution and reduced total and differential settlement for structures supported by a common foundation. For plants located at sites where the groundwater table is close to the surface and where dewatering to lower the groundwater table is not practical, the reinforcing steel for the mat foundation is protected against corrosion by using epoxy-coated reinforcing steel or a geosynthetic material is used to provide waterproofing function. The use of a geosynthetic material to protect the mat foundation creates a

weak interface which is more susceptible to shear and foundation sliding failure under strong earthquake motions. Earthquake motion may also cause uplift failure of the mat foundation. For sites with shallow bedrock, one of the techniques commonly used to eliminate sliding and uplift instabilities is the use of steel anchors to connect the mat foundation rigidly to the bedrock. The anchor is a tensile member and it is often very expensive to implement this technique. As stated earlier, most new NPP have significant component of the structure buried below grade. Therefore, the geotechnical engineers rely on section of the reinforced concrete walls embedded below grade to provide partial lateral resistance under passive soil condition to augment sliding resistance provided by the base friction.

Typically, regulatory limit on the acceptable foundation sliding will not allow the wall to undergo enough displacement to mobilize the maximum passive soil pressure. In some instances, it is either impractical or grossly uneconomical to design the embedded reinforced concrete walls for the maximum static and dynamic passive soil pressures. For this situation and where the maximum passive soil pressure is not mobilized, passive pressure methodology based on the soil deformation is required. The Mononobe-Okabe (M-O) equation developed in 1929 is the oldest method and most commonly used to evaluate the maximum earthquake-induced soil pressure on retaining walls. Equations 1 and 2 developed by Mononobe-Okabe are used to evaluate the coefficients of dynamic earth pressure under active and passive soil conditions, respectively.

$$K_A = \frac{\cos^2(\phi-\theta-\beta)}{\cos\theta\cos^2\beta\cos(\delta+\beta+\theta)\left[1+\sqrt{\frac{\sin(\phi+\delta)\sin(\phi-\theta-i)}{\cos(\delta+\beta+\theta)\cos(i-\beta)}}\right]^2} \qquad \text{Equation 1}$$

$$K_P = \frac{\cos^2(\phi-\theta+\beta)}{\cos\theta\cos^2\beta\cos(\delta-\beta+\theta)\left[1-\sqrt{\frac{\sin(\phi+\delta)\sin(\phi-\theta+i)}{\cos(\delta-\beta+\theta)\cos(i-\beta)}}\right]^2} \qquad \text{Equation 2}$$

$$\theta = \tan^{-1}\left[\frac{k_h}{1-k_v}\right] \qquad \text{Equation 3}$$

$$k_v = \frac{a_v}{g} \qquad \text{Equation 4}$$

$$k_h = \frac{a_h}{g} \qquad \text{Equation 5}$$

In Equations 1 to 5, i is the angle of inclination of the backfill soil with respect to the horizontal, δ is the interfacial angle between the wall and the soil, ϕ is the friction angle of the soil, β is the slope angle of wall with respect to the vertical, a_h and a_v are the horizontal and vertical components of earthquake-induced ground accelerations, respectively.

The M-O equation was developed for above grade retaining walls and one of the assumptions in its development is that the wall is flexible enough to generate minimum active soil pressure. This assumption does not apply to embedded structural walls which are considered rigid. Another assumption made in the development of the M-O equation is that the acceleration in all parts of the structure is the same. In the event of foundation sliding, the structural wall, sliding soil wedge, and stable soil base will have different acceleration values. This mechanism violates the assumption of same acceleration and the M-O equation becomes inappropriate (Enoki et. al., 2004). Dynamic soil pressure methodologies based on rigid plasticity theory such as the M-O equation have been reported to predict non-conservative results for embedded walls compared with solutions such as Wood (1975) which are based on elasticity theory. Most methodologies including those of Mononobe-Okabe (1929) and Wood (1975) did not consider dynamic properties of the soil and frequency of the earthquake motion.

One of the few methodologies available for evaluation of passive soil pressure based on the soil deformation was developed by Mokwa (1999). The methodology was based on results of field testing of reinforced concrete pile cap embedded at depths of between 1.5ft and 3ft. The equation (Equation 6) assumes that the piles are under static load and earthquake load was not considered.

$$P = \frac{y}{\left[\frac{1}{k_{max}} + R_f \frac{y}{P_{ult}}\right]} \qquad \text{Equation 6}$$

$$R_f = 1 - \frac{P_{ult}}{\Delta_{max} k_{max}} \qquad \text{Equation 7}$$

In Equations 6 and 7, P is the load capacity at a defined deformation, y; P_{ult} is the ultimate passive force; k_{max} is the initial stiffness; Δ_{max} is the deformation required to fully mobilize the passive force; and R_f is defined as the ratio between the actual failure force and the hyperbolic ultimate force.

The California Department of Transportation (Caltrans) adopted the results of study by Maroney (1995) to develop a series of load-deflection curves for seismic design of bridge abutments. The load–deflection curves were primarily based on Equation 8 which is empirical and only dependent on the area of the wall but did not consider soil-structure interaction effects, dynamic soil properties, and earthquake motion parameters.

$$P_{ult} = 5.0\,\text{ksf}\left[\frac{H}{5.5\text{ft}}\right]A_{wall} \qquad \text{Equation 8}$$

The existing methodologies discussed above are not appropriate for evaluation of deformation-based static and dynamic passive soil pressures for rigid embedded reinforced concrete walls.

The need for a methodology to evaluate static and dynamic passive soil based on the deformation is a major problem for most new NPP designs. To address this problem, a detailed finite element model of the soil-structure problem is typically developed. The finite element model is solved by developing linear and non-linear springs to represent the soil stiffness under static and dynamic loading condition. The deformation-based passive soil pressure is evaluated based on the reactions and strain developed in the springs.

Soil-structure interaction Problems

Typically, it is very computationally expensive to run a complete dynamic finite element model of the nuclear structures. A simplified but equivalent model of the structure and the soil is used in some cases. The equivalent static method involves development of a lumped mass model of the structure. The dynamic analysis of the

lumped mass model provides response spectra. Dynamic analysis of the lumped mass model depends on soil-structure interaction (SSI) effects.

SSI analysis is carried out to investigate how the presence of the structure influences the natural response of the soil deposits under earthquake. Dynamic SSI analysis is particularly important for heavy infrastructures such as nuclear power plants where the presence of the structure and/or deep excavations for foundation often have significant influence on the natural response of the soil. One of the most versatile and commonly used programs for SSI analysis is the System for Analysis of Soil-Structure Interaction (SASSI) which is developed and continuously being updated (SASSI2000) by Professor John Lysmer and his students at the University of California, Berkeley. SASSI operates in the frequency domain and assumes viscoelastic material properties. Therefore, it cannot incorporate soil and structural nonlinear effects which become very important under strong earthquake motions. Nonlinearity may result from dependence of soil behavior on the strain level and gap formation between the soil and the embedded wall.

SSI effects take two forms which are referred to as kinematic interaction and inertia interaction effects. Kinematic interaction effect is primarily related to the geometry of the structure and it is independent of the inertia properties of the structure. Kinematic effects tend to increase with the embedment of the structure. Kinematic effect tends to be negligible for most structures but for NPP with the mat foundation deeply embedded below grade, kinematic interaction effect is significant.

Inertia effect is dependent on the mass of the structure and the dynamic stiffness of the foundation soil. Commercially available computer programs such as ADINA and LS-DYNA which are capable of incorporating nonlinear effects in SSI analyses have not been adequately qualified by the NRC and are typically not acceptable for analyses of nuclear-related structures.

The geometry of the mat foundation for new NPP is irregular in most cases. Existing equations for computation of stiffness of foundation soil spring under both static

and dynamic condition were developed for common geometry like rectangular and circular shaped foundations. Therefore, the computation of soil spring stiffness using the methodology for rectangular or circular shaped foundation may be unacceptable. For nuclear structures where the mat foundation is neither circular nor rectangular, the dynamic soil spring stiffness is typically evaluated by assuming a rectangular or circular shaped foundation of the same area. The error introduced and the accuracy of this assumption is unknown. The distribution pattern for the foundation soil spring is also a challenge. For most NPP, the external walls will increase the rigidity of the mat foundation. This will results in contact pressure that has maximum values at the edges and minimum values at the center.

Stability of Foundation Supporting Soil

Bearing pressure imposed by the nuclear plant structures may exceed 50 ksf. Depending on the stiffness of the soil, this may lead to excessive total and differential settlement. Typical analysis of elastic settlement based on the Young modulus of the soil is excessive and unacceptable. Considering that the dimension of a typical mat foundation may exceed the size of a football field (360ft by 160ft) and more than 10ft in thickness, the use of the constrained modulus is considered appropriate for settlement analysis. Results of total settlement analysis based on the constrained modulus are more acceptable. Differential settlement between buildings supported on separate mat foundation is considered more significant because of buried pipes connected rigidly to adjacent structures. In most cases, the analysis of nuclear plants assumes limited horizontal variation in soil properties. As pointed our earlier, the containment structures typically impose higher bearing pressure and this generally lead to excessive differential settlement between buildings.

The geotechnical challenge is to develop a construction load sequence for all the structures at the site such that the differential settlement between the buildings is within acceptable limit. This is a very challenging task and requires input from the structural and construction engineering units.

References

Enoki, M., Luong, B.X., Okabe, N., and Itou, K. (2005)."Dynamic Theory of Rigid Plasticity", Soil Dynamics and Earthquake Engineering, Vol. 25, pp. 635-647.

Lysmer, J. et. al. (1981)."SASSI – A System for Analysis of Soil-Structure Interaction", Report No UCB/GT/81-02, Geotechnical Engineering, University of California, Berkeley

Lysmer, J. et. al. (1999)."SASSI200 – Theoretical Manual", Revision 1, Geotechnical Engineering, University of California, Berkeley.

Maroney, B. (1995)."Large Scale Bridge Abutment Tests to Determine Stiffness and Ultimate Strength under Seismic Load", Ph.D. Dissertation, Department of Civil Engineering, University of California, Davis

Mokwa, R.L. (1999)."Investigation of the Resistance of Pile Caps to Lateral Loading", Ph.D. Dissertation, Department of Civil Engineering, Virginia Polytechnic Institute and State University.

Mononobe, N. and Matsuo, H. (1929)."On the Determination of Earth pressures during Earthquakes", Proc. World Engineering Conference, vol. 9, pp. 176-182.

Wood, J.H. (1975)."Earthquake-Induced Pressures on a Rigid Wall Structure", Bulletin of New Zealand National Society for Earthquake Engineering, Vol 8(3), pp. 175-186

Ethanol Plant Supported on Aggregate Pier Foundation System

R. J. Franz, P.E., Division Manager, Hayward Baker Inc, Roselle, IL
RJFranz@HaywardBaker.com (630) 339-4300
A. L. Sehn, Ph.D., P.E., Chief Engineer, Hayward Baker Inc, Odenton, MD
ALSehn@HaywardBaker.com (410) 551-8200

ABSTRACT

Big River Resources, LLC has recently constructed a 100 MGPY (100 million gallons per year) ethanol production facility in Galva, Henry County, Illinois. Geotechnical explorations for the project reported the presence of relatively deep deposits of compressible, high moisture, organic silty lean clay. The project geotechnical engineer recommended ground improvement with aggregate piers for support of the more heavily loaded plant structures, in particular the tanks and process equipment.

Hayward Baker Inc. was hired by Big River Resources to provide ground improvement with Vibropiers. HBI installed 30-inch and 36-inch diameter Vibropiers to 10 to 15 feet below the working grade for support of the beer well, fermentation tanks, process area structures, energy center, cooling tower, tank farm and water treatment facilities.

The paper presents the site conditions and design of the aggregate pier system to increase bearing capacity and reduce expected settlements to tolerable levels. QA/QC procedures and verification testing are also presented.

GEOLOGY

Based on a review of the Henry County, Illinois Soil Survey, the soils in the project area are primarily composed of Oakville-Tell-Waukegan Association materials. The soils were deposited as glacial outwash plains, capped with loess. The soils in this association are characterized by fine sands, silty loams, loamy silts, and sandy loams. The soils in this association are typically poorly drained, and the loams contain trace to moderate amounts of organic materials (Elmer, 2004; Terracon, 2007).

On the project site, the soils consisted primarily of lean to fat clays, silty clays, clayey silts and sandy clays. A layer of organic clay was identified beneath many of the plant structures. The organic clay, in particular, exhibited low strength and high compressibility.

Underlying the unconsolidated deposits, at depths of approximately 30 to 40 feet below original ground surface, bedrock was encountered consisting primarily of slightly weathered shale, with intermittent layers of limestone, sandstone, and siltstone, as well as some scattered coal seams. An idealized soil profile at the plant site is presented in Figure 1.

FOUNDATION LOADS AND PERFORMANCE REQUIREMENTS

Foundations for the ethanol production facility typically consisted of ringwall footings with engineered in-fill for tank structures; and conventional square and rectangular spread footings and mats for buildings, process equipment, process tanks and cooling structures.

Applied foundation pressures were designed to range from approximately 500 psf to over 5,000 psf. Allowable total settlements ranged from ½ inch for drum dryers and duct foundations to 2¾ inches for fermentation tanks. Allowable differential settlements ranged from ¼ inch for the dryers to 1¼ inches for liquefaction and other feed tanks.

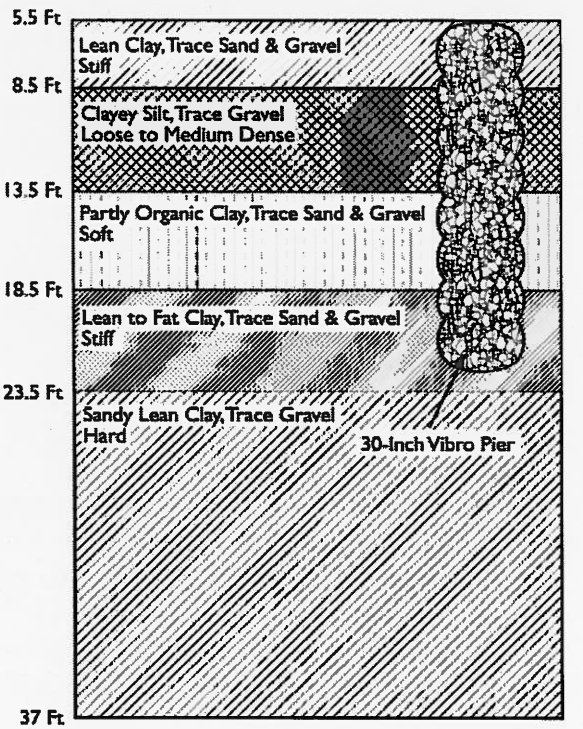

FIGURE 1 Idealized soil profile.

AGGREGATE PIER DESIGN ISSUES

Design of an aggregate pier system involves the same basic considerations as the design of any other foundation system – strength, serviceability, and economics. The strength aspects of the design generally involve an evaluation of the bearing capacity of the foundation soils improved by the aggregate piers, and an assessment of the ability of the soil surrounding the aggregate piers to provide lateral support and confinement of the aggregate pier.

Soil Properties

The soil properties required to complete the aggregate pier design are the same as those required for the bearing capacity and settlement design of a typical shallow foundation system. The designer must be able to estimate the strength and stiffness of the soil strata that are within the stress influence zone of the foundation and aggregate pier system. For cohesionless soils, the soil properties are typically estimated using empirical correlations and the results of insitu test methods such as SPT or CPT testing. This approach is also commonly applied to cohesive soils. For cohesive soils, index property testing and laboratory testing to determine strength and compressibility are also desirable.

Aggregate Pier Properties

As with any cohesionless granular soil, the strength and stiffness of the aggregate pier are primarily dependant upon the stress condition and the engineering properties of the particular aggregate used to construct the aggregate pier. Of particular interest are the friction angle and the elastic modulus of the aggregate pier material. The two most common aggregate gradations

are AASHTO #57 and dense-graded aggregate materials similar to the VDOT 21b (Illinois CA-6) gradation. Both gradations are widely available as crushed stone. The gradation requirements for the #57 and 21b gradations are listed in Table 1.

A detailed investigation of the shear strength and stiffness properties of four different crushed rock aggregates was reported by Duncan et al., 2007. The study involved 6-inch-diameter triaxial shear strength testing of two aggregates with #57 gradation and two aggregates with 21b gradation. Each aggregate was tested at two different relative density ranges, and effective confining pressures ranging from 3.7 to 30.5 psi were used. Specimens were prepared using one of two different compaction energies. The "High Test Density" specimens were compacted using a Standard Proctor compaction hammer and the Standard Proctor compaction energy of 12,400 ft-lbs per ft^3. The "Low Test Density" specimens were prepared with minimal compaction effort.

TABLE 1 Gradation Requirements for the AASHTO #57 and VDOT 21b Gradations

	Amounts Finer than each Laboratory Sieve (square openings) (% by mass)									
Gradation No.	2.0 in.	1.5 in.	1.0 in.	0.5 in.	0.375 in.	No. 4	No. 8	No. 10	No. 40	No. 200
57	- -	100	95-100	25-60	- -	0-10	0-5	- -	- -	- -
21b	100	- -	85-95	- -	50-69	- -	- -	20-36	9-19	4-7

The data reported by Duncan et al., 2007 indicate a clear pronounced increase in the measured friction angle with decreasing effective confining pressure. This indicates that it is important to consider the level of confinement when selecting strength parameters for design. The influence of effective confining pressure on measured friction angle also helps to explain why a relatively wide range of friction angles are often cited for these materials. The very high values are generally only applicable at the lower range of effective confining pressures. The influence of effective confining pressure on friction angle is often expressed in the form:

$$\phi' = \phi'_0 - \Delta\phi' \log\left(\frac{\sigma'_3}{p_a}\right) \qquad \text{eqn. 1}$$

where ϕ' = effective stress friction angle, σ_3' = effective minor principal stress, ϕ_0' = effective stress friction angle for $\sigma_3' = p_a$, $\Delta\phi'$ = decrease in ϕ' for a tenfold increase in σ_3', and p_a = atmospheric pressure expressed in the same units as σ_3'. Using this approach, the results of the testing reported by Duncan et al. are summarized in Table 2.

Based on the results presented by Duncan et al., crushed rock materials with 21b and #57 gradations both exhibit high frictional strength. These materials are both well suited for the construction of aggregate pier systems, and the use of friction angle values in the 45 to 55 degree range is justified.

TABLE 2 Frictional Properties for Crushed Rock Aggregate with 21b and #57 Gradations Tested at Two Density Ranges (after Duncan et al., 2007)

Aggregate Gradation	Test Density	ϕ_0' (degrees)	$\Delta\phi'$ (degrees)
21b	"Low"	44	10
21b	"High"	53	12
#57	"Low" and "High"	48	11

BEARING CAPACITY DESIGN OF AGGREGATE PIER SYSTEMS

The aggregate pier system is a complex soil-structure interaction case. The shallow footing element applies stress to the soil-pier system, and the response of the pier is influenced by the engineering properties of the pier itself and by the engineering properties of the surrounding soil. One aspect of this interaction is the maximum vertical stress that the aggregate pier can sustain before shear stresses within the pier exceed the shear strength of the aggregate pier material. The stress state in the pier is similar to that in a conventional triaxial shear. As vertical load is applied to the aggregate pier, it will experience compressive strains in the vertical direction and extension strain in the lateral direction. This lateral strain mobilizes the passive resistance of the soil surrounding the aggregate pier and increases the confining stress on the aggregate pier. The aggregate pier can be considered an expanding body within the matrix soil. Brauns (1978) represented this problem as shown in Figure 2 and developed a solution to the problem. Additional details on Braun's method and a convenient chart-based method of applying it were reported by Sehn and Blackburn, 2008.

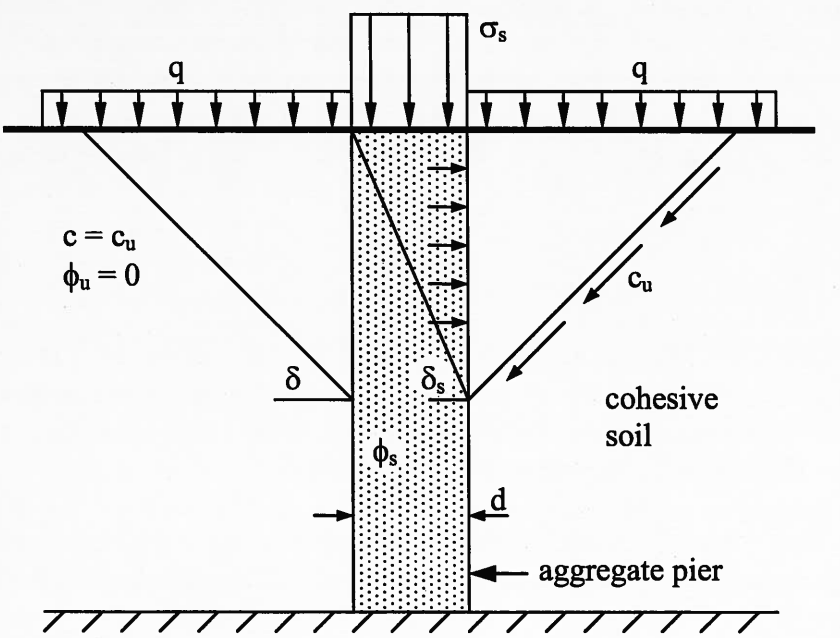

FIGURE 2 Ultimate capacity of an aggregate pier in cohesive soil (after Brauns, 1978).

SETTLEMENT ANALYSIS OF AGGREGATE PIER SYSTEMS

In order to estimate the foundation settlements, consideration must be given to settlements resulting from compression of the upper zone and those resulting from compression of the lower zone. The upper zone is the zone reinforced by the aggregate piers, and the lower zone is the soil layers below the bottom of the aggregate pier treatment zone. The foundation settlement is the sum of the upper zone settlement and the lower zone settlement.

Upper Zone Settlement

In the US, the most commonly used method for evaluating the upper zone settlement is the spring analogy (Lawton et al., 1994). In the spring analogy, the behavior of the soil and that of the aggregate piers is taken to be linear and elastic. The stiffness of the soil is represented by the soil reaction modulus, and the stiffness of the aggregate pier is represented by the pier reaction modulus. It is important to note that these parameters are not 'true' moduli, quantifying a stress-strain relationship, but are nominal stiffness values reflecting the vertical load-displacement relationship. These two modulus values are subgrade reaction moduli, and are defined as follows:

$$K_p = \frac{q_p}{\delta_p} = \textit{pier reaction modulus} \qquad \text{eqn. 2}$$

$$K_s = \frac{q_s}{\delta_s} = \textit{soil reaction modulus} \qquad \text{eqn. 3}$$

where: q_p = bearing pressure on the aggregate pier
q_s = bearing pressure on the soil
δ_p = settlement of the aggregate pier caused by q_p
δ_s = settlement of the soil caused by q_s

Considering vertical force equilibrium and displacement compatibility, the following equation can be written:

$$q_p = \frac{q\left(\frac{K_p}{K_s}\right)}{\left(\frac{A_p}{A}\frac{K_p}{K_s} - \frac{A_p}{A} + 1\right)} \qquad \text{eqn. 4}$$

where: q = footing average bearing pressure
q_p = bearing pressure on the aggregate pier
A = total footing area
A_p = total aggregate pier area
A_s = soil area ($A - A_p$)

In the design of aggregate piers, equation 4 is used to calculate the stress applied to the aggregate pier. Combining this value of aggregate pier stress with the aggregate pier reaction modulus, the expected settlement can be calculated using equation 2. For aggregate piers beneath spread or strip footings, the area treatment ratio A_p/A is typically in the 0.25 to 0.45 range, depending on the improvement required.

The soil reaction modulus can be estimated by evaluating the expected settlement for a footing loaded to a particular bearing pressure supported on the soils at the site without using any aggregate piers. This calculation is done using conventional geotechnical settlement calculations for shallow foundations. The soil reaction modulus can then be calculated as the bearing pressure divided by the predicted settlement.

The aggregate pier reaction modulus depends on the strength and stiffness of the soils at a particular site and on the properties of the aggregate pier. An aggregate pier modulus test is often conducted at the start of construction in order to verify the accuracy of the modulus value used in design. Additional details on the design method and guidance on selecting soil and pier modulus values are contained in the paper by Sehn and Blackburn, 2008.

Lower Zone Settlement

Estimating the settlement that will result from compression of the soil layers below the zone treated by the aggregate piers can be done using a variety of applicable methods from conventional foundation design. This may involve an evaluation of elastic settlement if the underlying soils are cohesionless, or an evaluation of primary consolidation and secondary compression settlements if the underlying soils are cohesive. In either case it will be necessary to: a) characterize the compressibility of the soils below the depth of treatment and b) determine the stress increase resulting from the applied loading. The evaluation of compressibility of the soil layer(s) is done the same way as for any other foundation settlement evaluation (consolidation tests, pressuremeter tests, or some other test or empirical correlation method).

Evaluation of the increase in vertical stress below the improved zone is less straightforward because of the complex nature of the interaction between the footing, the aggregate piers, and the surrounding soil. Based on numerical analyses and an evaluation of existing methods for predicting the stress increase below the aggregate pier zone, Sehn and Blackburn, 2008 recommended the use of the modified pier group method for calculating the increase in vertical stress in the lower zone. The method is adapted from the methods commonly used to evaluate stresses below pile groups and is represented graphically in Figure 3.

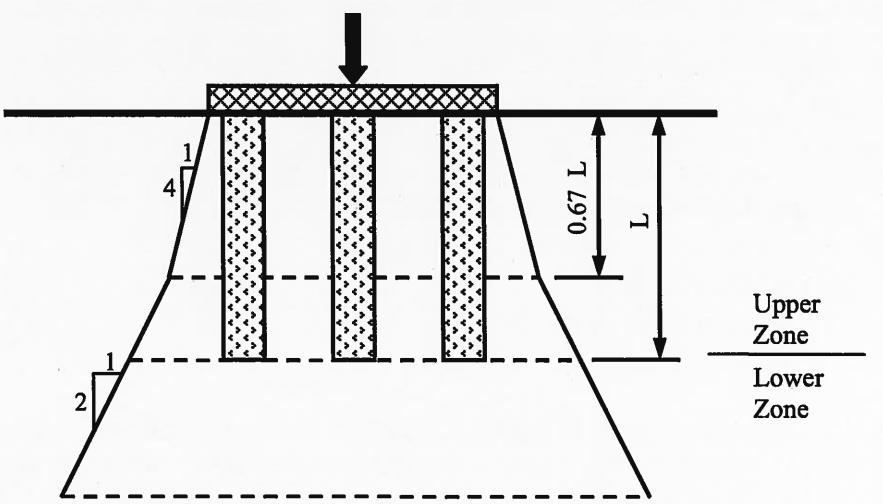

FIGURE 3 Modified pier group method for calculating the change in vertical stress below the aggregate pier treatment zone.

PROJECT DESIGN SUMMARY

The objective of HBI's ground improvement design was to reduce settlement of the compressible slightly organic materials to within the design criteria. The potential settlement of the deeper hard, sandy lean clays and dense silts with clay was determined to be negligible.

The ground improvement design generally consisted of 30-inch diameter aggregate piers which extended to depths of 10 to 15 feet below the working grade. For the heavily loaded distillation area, 36-inch diameter elements were installed to better manage settlement and stress concentrations on the piers. The design was subdivided into specific component areas of the plant for convenience. A summary of the basic design is presented in Table 3.

INSTALLATION METHOD

The aggregate piers were installed using the pre-drilled, dry, top-feed (Vibro Pier) method. Both 30-inch and 36-inch diameter cavities were excavated with excavator-mounted auger drills. The down-hole vibrator was then inserted to the bottom of the hole and coarse aggregate materials introduced around the vibrator annulus. The aggregate was then densified in lifts as the aggregate was vibrated and re-penetrated by the vibrator. The vibrator itself weighs approximately 3 tons and employs the rotation of internal, eccentric weights to exert approximately 25 tons of centrifugal force on the surrounding aggregate and soil matrix. The equipment used to install the aggregate piers is shown in Figure 4.

TABLE 3 Summary of Aggregate Pier Designs for the Various Buildings and Tanks

Plant Area or Component	Aggregate Pier Diameter	Aggregate Pier Length	Aggregate Pier Spacing
Fermentation Tanks and Beer Well	30-inch	15 feet	8 foot square grid plus ring walls
Exterior Process Tanks	30-inch	12 feet	8 foot square grid plus ring walls
Process Building – Footings	30-inch	10 feet to 15 feet	1 to 4 per foundation
Process Building – Mats	30-inch	15 feet	8 foot square grid
Process Building – Distillation Area	36-inch	15 feet	8 foot square grid plus supplements at concentrated loads
Energy Center – Building Columns	30-inch	15 feet	2 to 3 per foundation
Energy Center – Equipment Mats	30-inch	15 feet	7 foot square grid
Cooling Tower	30-inch	15 feet	10 foot square grid
Tank Farm	30-inch	15 feet	7 foot square grid
Water Treatment	30-inch	15 feet	6 foot square grid plus ring walls and 3 to 6 per footing / mat

FIGURE 4 Crane, loader, and pre-drill rig being used to install aggregate piers.

QC/QA

Quality Control and Quality Assurance for Vibro Pier installation had several components. Each Vibro Pier location was marked in position in the field with a numbered pin flag by a land surveyor. During excavation, a log of hole depth was maintained by HBI and Terracon personnel, confirming each hole location and its corresponding required design depth. The approximate volume of aggregate placed in each Vibro Pier was logged and confirmed to exceed the theoretical volume of the pier. The maximum amperage drawn by the vibrator for each lift of aggregate placed was also recorded. A minimum threshold amperage was established and the minimum amperage measured before the vibrator would be extracted. Volume and amperage were logged by both Terracon and HBI personnel.

LOAD TESTING

Two load tests were conducted during the ground modification work. Tests were performed on a 36-inch diameter Vibro Pier constructed in the Distillation Area of the Process Building and on a 30-inch diameter Vibro Pier constructed in the Cooling Tower area. The data presented below depicts one of the tests, each of which was representative of the Vibro Pier installation in terms of both column geometry and representative subsurface conditions across the site. The data shown in Figure 5 represent an assessment for a 47 kips service load on the aggregate pier.

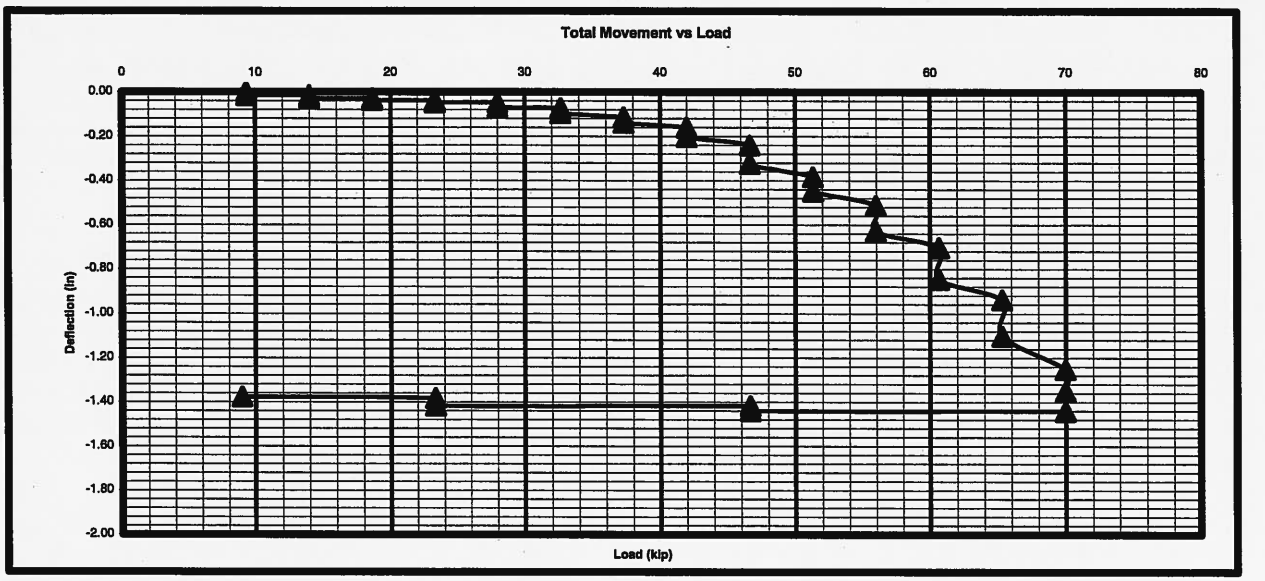

FIGURE 5 Results of a typical modulus load test.

SUMMARY

Aggregate piers are becoming a widely used intermediate foundation system to increase the bearing capacity and reduce the settlement of shallow foundations for sites with marginal soils. The design of these systems involves an evaluation of the settlements resulting from compression of the aggregate pier reinforced layer (upper zone) and from compression of the soil layers below the aggregate pier treatment depth (lower zone). Reasonable estimates of the stress increase in the lower zone are critical in making accurate predictions of the expected settlements.

Based on the data reported by Duncan et al. (2007), there is only a very minor difference between the strength of #57 crushed aggregate and 21b (DGAB) crushed aggregate. Either aggregate gradation is capable of producing friction angles in the 45 to 55 degree range. The friction angle of both gradations was found to be influenced by the effective confining pressure to a significant degree.

Ethanol is likely to continue to play a role in the energy infrastructure of the United States. The placement of ethanol production facilities near the source of feedstock means that local geologic conditions will play a significant role in the design and construction of each individual plant. As presented in this paper, aggregate piers ground modification techniques can be an effective method to manage foundation performance for project sites underlain by compressible soil deposits.

Big River's Galva facility began production in early June 2009 and had its official ribbon cutting September 14, 2009.

REFERENCES

ASTM C 33 – Standard Specification for Concrete Aggregates. *2007 Annual Book of ASTM Standards*, Section 4, Volume 04.02 Concrete and Aggregates.

Brauns, J. (1978). "Die Anfangstraglast von Schottersaulen im bindigen Untergrund." *Die Bautechnik*, 8/1987.

Duncan, J. M., Brandon, T., Jian, W., Smith, G., Park, Y., Griffith, T., Corton, J., Ryan, E. (2007). *Densities and Friction Angles of Granular Materials with Standard Gradations 21b and #57.* Center for Geotechnical Practice and Research, Virginia Tech, Report No. 45, August, 2007.

Elmer, S.E. (2004). Soil Survey of Henry County, Illinois, Natural Resources Conservation Service, United States Department of Agriculture.

Fagen, Inc. / Fagen Engineering, LLC, BRGA CC Found ----07.dwg, various dates.

Fagen, Inc. / Fagen Engineering, LLC, Tank and Vessel Weights by Area for a 100 magpie Plant, BURR – Galva, Illinois, undated.

Lawton, E. C., Fox, N. S., and Handy. R. L. (1994). "Control of Settlement and Uplift of Structures Using Short Aggregate Piers." *In-situ Deep Soil Improvement*, Geotechnical Special Publication No. 45, ASCE, New York, pp. 121 – 132.

Sehn, A. L. and Blackburn, J. T. (2008). "Predicting Performance of Aggregate Piers," Proceedings of the 23rd Central Pennsylvania Geotechnical Conference, May 28-30, 2008, Hershey, PA.

Terracon Consultants, Inc., Geotechnical Engineering Report, Proposed Ethanol Production Facility, Route 34 and Industrial Avenue, Galva, Illinois, April 4, 2007, Terracon Project No. 11065244

VDOT – Virginia Department of Transportation (2002). *Road and Bridge Specifications*, Section 208, Subbase and Aggregate Base Material.

Evaluation of Voids within an Earthen Embankment

By

Scott J. Ludlow, Ph.D., P.E.[1]

ABSTRACT: The Sturgis Hydroelectric Project was built in 1910 under a permit by the War Department and is located 120 mi from the mouth of the St. Joseph River near Centreville, Michigan. The City of Sturgis owns and operates the dam and associated facilities under a Federal Energy Regulatory Commission license. The facility consists of four hydroelectric generators housed in two separate powerhouses, a concrete arch dam/spillway, an earthen embankment, and an auxiliary spillway. The earthen dam is approximately 500 ft long with a structural height of about 23 ft, sideslopes of 2-horizontal to 1-vertical upstream and 2½-horizontal to 1-vertical downstream, and a 10-ft wide berm 20 ft down slope of the crest.

During a previous grouting program, suspected voids were filled to reduce seepage at the face of an existing abutment. The volume of grout injected during the program indicated that the extent of the voids might be considerably larger than anticipated. Another item of interest, which was not part of the previous grouting program, included an additional area of seepage located south of the abutment and near the toe of the downstream embankment slope. To understand the extent of the voids and address areas of seepage, a ground penetrating radar survey was performed. Results of the survey were used in support of remedial measures and depicted toe/lateral drains and the interpreted presence of voids and perched water near the seepage areas. This paper presents the results of the survey and remedial measures taken to arrest the seepage.

PHYSIOGRAPHIC AND GEOLOGIC SETTINGS

The facility is situated in the Northern Lake and Moraine Region and is characterized by thick deposits of morainal and outwash deposits within a topographic valley of the St. Joseph River. Glaciers have shaped the contemporary landscape as well as left deposits that make up the surficial geology in the St. Joseph River basin of southwest Michigan and northeast Indiana. During the Wisconsinan stage of glaciation in the Pleistocene Epoch (10,000 to 75,000 years ago), most of Michigan and Indiana were covered by several ice lobes (Farrand and Eschman, 1974). The St. Joseph River basin was an interlobate region; its landscape being shaped by three glacial lobes. The Saginaw lobe came from the northeast, the Erie lobe from the east, and Lake Michigan lobe from the northwest. The St. Joseph River flowed south into the Kankakee River and then the Mississippi River and the Gulf of Mexico. During glacial retreat, water was no longer forced by the wall of ice to flow down to the Kankakee River. Therefore, a new

[1] Principal Engineer, Earth Exploration, Inc., 7770 W. New York St., Indianapolis, IN 46214. E-mail: sludlow@earthengr.com

channel with less water resistance was formed, and the flow changed to a northward direction at South Bend, downhill to the now lower elevation Lake Michigan. The glacial retreat also left varied moraine and outwash deposits that strongly influence the local hydrology, channel morphology, and gradient of the mainstem and tributaries. As such, the basin consists of a mosaic of outwash sands, ice contact material (unsorted sands and gravel), coarse end moraine (sands and gravel), fine end moraine (loamy), and lake plain (Lineback et al. 1983).

PROBLEM DEFINITION

During 2000, a grouting program was implemented to fill suspected voids and thereby reduce seepage at the face of the existing south abutment for the concrete arch spillway. The volume of grout injected during the program indicated that the extent of the voids might be considerably larger than anticipated although seepage diminished. Another item of interest, which was not part of the grouting program, included an additional area of seepage located south of the abutment and near the toe of the downstream embankment slope. To understand the extent of the voids and address areas of seepage, consideration was given to a ground penetrating radar (GPR) survey.

GPR METHOD DESCRIPTION

GPR is a non-intrusive geophysical method that is capable of detecting natural and manmade features in the subsurface environment. The method uses a transmitting antenna to radiate high frequency (typically 50 to 1,500 MH) electromagnetic pulses into the subsurface. Subsurface objects reflect some of the incident electromagnetic energy back to the surface where it is detected by a receiving antenna. A continuous record of these reflected signals is used to map the spatial distribution of subsurface features.

Radar Energy Propagation

The total energy of the transmitted pulse is diminished as it travels through the subsurface materials. Attenuation is a primary source of energy loss and is a direct function of the frequency of the radar signal and the physical properties of the subsurface materials. Greater attenuation occurs at higher radar frequencies and in materials with higher electrical conductivity, higher magnetic susceptibility, and lower dielectric permittivity. The presence of ground water or clay minerals in soil or bedrock results in decreased depths of penetration. Conversely, greater depths of penetration are achieved in dry sand and gravel units. Other factors that result in energy loss include absorption (the conversion of radar energy to heat), scattering and clutter, and spherical divergence (the geometrical spreading of a finite amount of energy through larger volumes with increasing depth).

Some of the incident energy is reflected at a material boundary, and the rest is transmitted through the boundary. The magnitude of the reflected energy is a function of the contrast in the permittivity of the host material and the target reflector (permittivity is expressed in terms of the dielectric constant). The amount of energy reflected at a material boundary (for a normal incident wave) is quantitatively expressed as:

$$R = \sqrt{\varepsilon_U} - \sqrt{\varepsilon_O} / \sqrt{\varepsilon_U} + \sqrt{\varepsilon_O}$$

where R is the reflection coefficient, ε_O is the dielectric constant of the overlying material, and ε_U is the dielectric constant of the underlying material. Using extreme values for dry (ε_O = 3) and saturated sand (ε_U = 30), a reflection coefficient (R) of 0.52 is calculated; indicating that 52% of the downward traveling energy is reflected, and 48% is transmitted through the boundary. This demonstrates the importance of water (ε_U = 81%) in the pores of the geologic material. When all else is equal, more energy will be reflected from saturated geologic materials, geologic deposits that contain more water due to a greater bulk pore volume, and clay minerals that contains water in its lattice structures.

The strength of the reflection is also dependent on the sharpness or abruptness of a geologic boundary. This will affect the ability to image the depth of saturation (phreatic surface) in finer-grained deposits, such as fine to medium sand or silt. Due to capillary forces in these materials, the phreatic surface will consist of a gradual transition from saturated to unsaturated soil in the fine pores. This gradual increase in water content will result in the gradual reflection of incident energy. Different frequencies will be reflected at differing depths of saturation, resulting in dispersion of the radar signal. If the capillary zone is broad enough, its reflection will be indistinguishable on the radar record.

The vertical resolution achievable with GPR is determined by the frequencies that compose the radar signal. The minimum vertical dimension that can be resolved (in theory) is 7 equal to one quarter of the signal wavelength, which is dependent on the signal frequency and the velocity of the medium. These parameters are related by the following equations:

$$\lambda = V/f \qquad \text{and} \qquad V = C/\sqrt{\varepsilon}$$

Therefore, the minimum resolvable vertical dimension is:

$$\lambda/4 = C/4f\sqrt{\varepsilon}$$

where λ is the wavelength, v is the velocity of the electromagnetic energy through the material, f is the frequency of the radar signal, ε is the dielectric constant of the material, and C is the speed of light. In summary, vertical resolution increases with lower velocity and greater permittivity, and therefore greater moisture content.

Presentation of Radar Data

The recorded radar signals are graphically displayed on a chart, as shown in Figure 1. The horizontal axis of the chart represents the profiled distance. The vertical axis of the chart represents the two-way travel time for the radar signal (i.e., the time required for the signal to travel to a reflector and back to the surface). Planar and flat-lying subsurface features are generally represented on the record as multiple horizontal reflections. Planar, sloping features are generally represented as multiple sloping reflections. Objects, such as drains, pipes, and cobbles may cause the diffraction of the radar signal; they are depicted in the graphic record as hyperbolas with the apex of the hyperbola located at the source of diffraction. The slope of the limbs of the hyperbola is a function of the velocity of the subsurface material. Estimates of the radar velocities from analysis of diffraction hyperbolas can be used to depict average depths along the

vertical axis. However, such velocity measurements must be used with caution because velocities typically vary laterally and with depth as a result in changes in soil types and their moisture content.

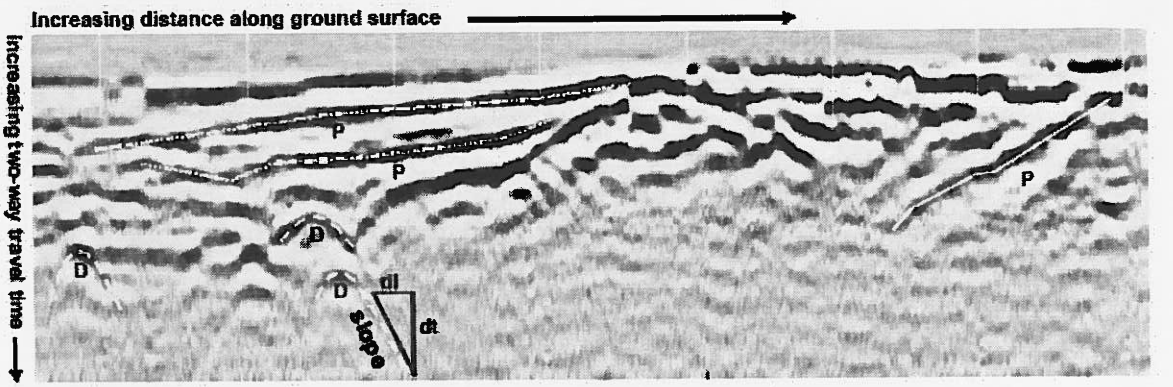

Figure 1. Typical Radar Section

The profile depicts planar bedding (as dotted lines marked P), diffraction hyperbolas (as curved lines marked D), and other dipping reflectors (unlabeled). The limbs of the diffraction hyperbolas have a slope related to the average velocity of radar energy through the soil interval between the antenna and the point of diffraction. Horizontal distances are incremented by faint vertical lines or distance markers; the distance between markers may vary between profiles. The vertical axis shows two-way travel time measured in nanoseconds. Estimates of the radar velocities (from analysis of diffraction hyperbolas) can be used to depict depth (e.g. in ft) along the vertical axis.

DATA ACQUISITION AND PROCESSING

Radar Profiles Established by Survey

Prior to the GPR data collection activities, the radar profile locations were staked and surveyed, and wire flags were placed at 25-ft intervals in the longitudinal direction (north to south) of the dam, along the furthest eastern and western profile lines. In the transverse direction, flags were placed at 3-ft intervals down the embankment slope (east to west) at every fourth flag (every 100 ft), and at 6-ft intervals at intermediate points (25, 50 and 75 ft). In addition to the staking activities, Elevations of the profiles at 50-ft intervals were also established.

Ambient Site Conditions

Radar data were collected in January and February 2001. At that time, the surface of the dam was covered with variable amounts of snow that was in the process of melting. In January, most of the embankment was covered with snow; by February, there were large snow-free areas. Ground water elevation measurements of piezometers were collected by others in January and were made available for use during the processing and interpretation of the radar data.

Antenna Selection

Two monostatic antennas of differing frequencies were tested to determine which would provide the optimum balance between the depth of penetration and subsurface resolution. (Note that each monostatic antenna served as both the transmitting and receiving unit.) While the 80- MHz antenna can penetrate deeper into the subsurface, the resolution of the antenna is relatively low for the anticipated site conditions ($\lambda/4 \cong 15$ in.). Conversely, the 300-MHz antenna will not penetrate as deeply, but has greater resolution ($\lambda/4 \cong 4$ in.). Transverse profiles were collected with both antennas and the 300-MHz antenna was found to have an estimated maximum depth of penetration of 18 ft, which was determined adequate for the survey.

Data Acquisition

Following the evaluation of the radar antennas, survey data were acquired along longitudinal profiles and then along transverse profiles. Data were collected with a Geophysical Survey Systems SIR-2 system and the 300-MHz (megahertz) antenna. The SIR-2 system allows the collection, recording and processing of continuous, digitally sampled radar data. The data acquisition parameters were as follows:

bits/sample	16	16-bit samples are better suited when advanced processing methods may be needed.
samples/record	1024	Sampling rates directly influence the bandwidth and vertical resolution.
records/second	24	Spatial sampling rate directly influences the horizontal resolution.
record length	300×10^{-9}sec	Record lengths dictate the maximum depth of imaging and coupled with sampling rate, determine the vertical resolution.
traces stacked	2 traces	Trace stacking adds two or more traces to form one composite trace, thereby reducing high frequency noise.
high pass filter	85 MHz	High pass (low cut) filtering removes low frequency waveforms that can cause clipping of superposed, high frequency waveforms.

Gain settings were established each time that the instrument was restarted, which was typically several times per day. Gain control is used to amplify the recorded (reflected) signal to compensate for energy loss with depth. The gain function that is automatically generated by the instrument calculates an optimum curve for a fixed time interval. That gain curve was manually overridden to assure that the recorded data would stay within the dynamic range of the instrument and clipping would be held to a minimum.

Care was taken during each profile to minimize disturbance to the snow cover because variations in the snow thicknesses could result in variations in the arrival times of subsurface reflections. Because the radar antenna tended to slide downhill along both the longitudinal and transverse profiles, a rope tether was used to gain greater control of the path and orientation of the antenna.

Radar data were collected along 50 longitudinal and 68 transverse profiles. Longitudinal profiles were more densely spaced in areas of greater interest (i.e., near the south abutment wall and the zone of seepage). A 3-ft profile interval was used on the southern portion of the dam (0 to 300 ft south of the south abutment wall), and a 6-ft interval was used on the northern portion of the dam (300 to 460 ft south of the south abutment wall). Similarly, transverse profiles were spaced at 3-ft intervals from 0 to 150 ft south of the south abutment wall, and at 25-ft intervals over the remainder of the dam. As radar data were collected, distance markers were added to the data set at even increments (flagged locations of profile intersections). The markers provide geographic reference points that are later used to tie the radar data to known points on the dam.

Data Processing

Distance Normalization: The SIR-2 radar system collects data at a constant rate of records per second, so variations in the traverse speed of the antenna will result in variations in the number of records per unit distance. For example, a slow-moving antenna will take more time to traverse a fixed distance, and more records will be recorded over that distance. As a result, the distance markers (representing evenly-spaced intervals) appear to be erratically spaced in the records.

Data normalization corrects for changes in antenna speed by a process known as Érubber sheeting,Êwhich is a linear extrapolation between known distance markers. The resulting records exhibit evenly spaced distance markers that are consistent from record to record.

Gain Restoration: Variations in the gain function occurred as ambient field conditions changed. Because there was no practical standard on which to base a constant gain setting over time, all gain functions established during acquisition were removed (the data were restored to a no gain state), and a consistent gain function was employed for all records. The gain settings applied in the field served the purpose of providing enough gain to view deeper reflections during acquisition while largely avoiding clipping of the high amplitude reflections. Figure 2 shows the effects of gain restoration for a record collected down the embankment slope.

Frequency Filtering: A high pass filter was applied to the records after gain restoration to remove the horizontal banding that is attributed to system noise and is inherent in the radar method (Figure 3). Additionally, this filter removed noise deeper in the section that was an artifact of the gain restoration step. While frequency filtering does not perfectly remove horizontal banding due to system noise, it does not remove horizontal reflections from flat-lying soil units; more aggressive methods that are commonly used to remove banding often obliterated these desired reflections.

Velocity Estimation through Migration: Selected radar data were analyzed to estimate average radar wave velocities through the dam. By calculating soil velocities, the depths of features observed in radar records can be estimated from their two-way travel times (described in Section 3.2). Migration is a process that redistributes diffracted energy that results from scattering by point sources and abrupt discontinuities in the subsurface. Diffracted energy is evident in radar records as inverted hyperbolas. The slopes of the hyperbola limbs are a function of the radar velocity in soil (see Figure 4).

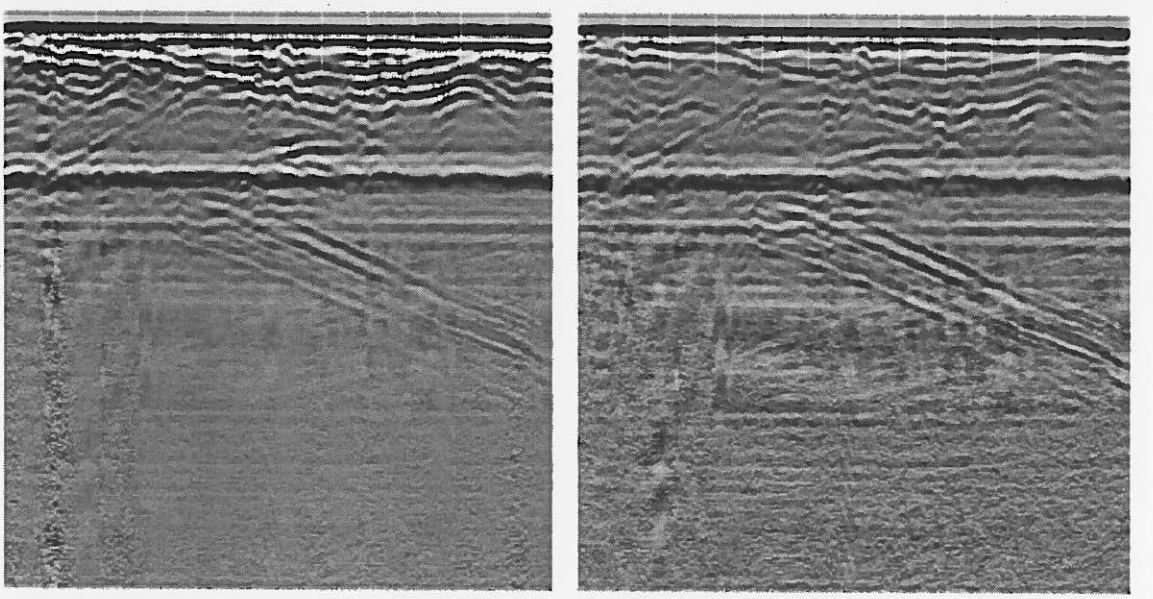

Figure 2. Gain Restoration

Radar file before (left) and after (right) gain restoration. Note the consequent reduction in the number of shallow, high amplitude reflections (white and black bands), the greater amplitude of deeper reflections, but increase in noise with depth.

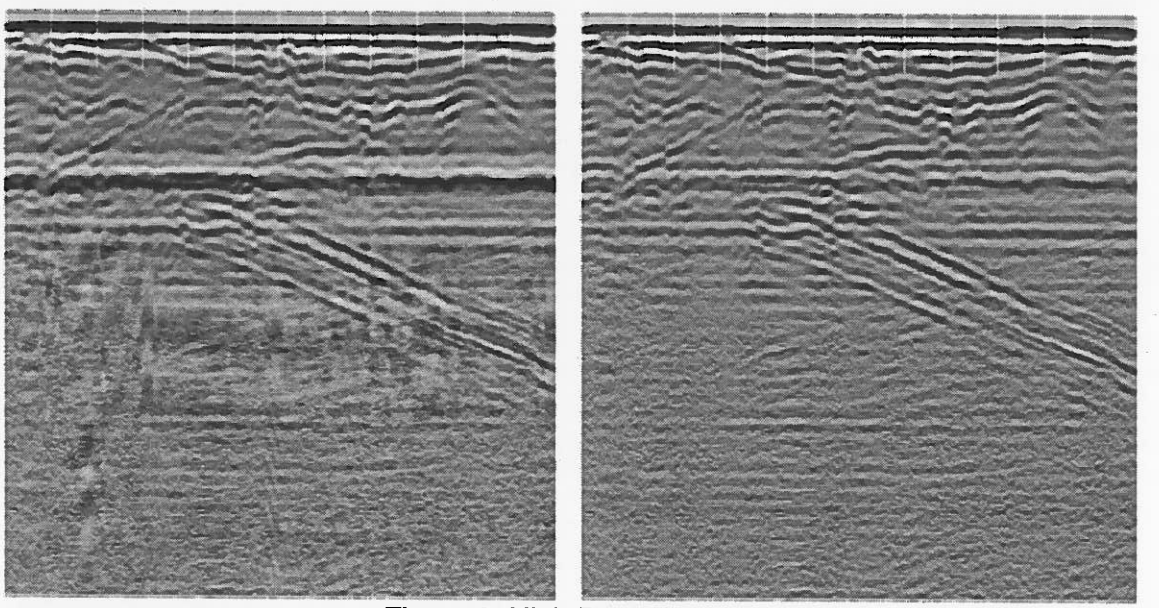

Figure 3. High Pass Filtering

Radar file before (left) and after (right) high pass frequency filtering. Note the consequent reduction in both the horizontal banding (system noise) and noise imparted by gain restoration. Horizontal banding can be mistaken as reflections.

When the correct velocity is used for migration, diffracted energy will be concentrated at a single point; incorrect migration velocities will result in over- or under-migrated energy. Note that the migration processes results in an average velocity for the soil between the antenna and the point of diffraction.

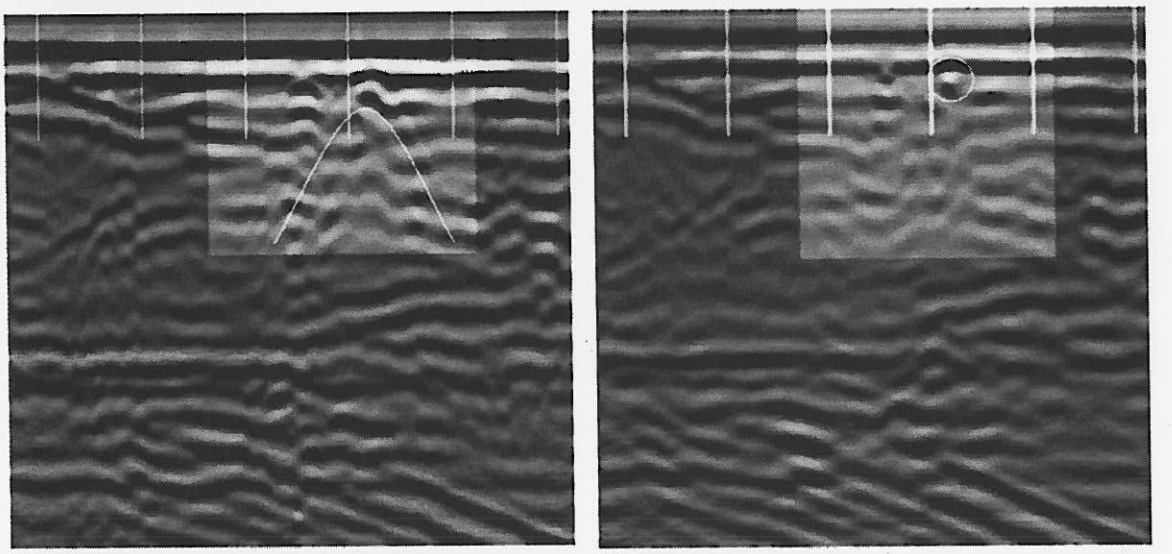

Figure 4. Velocity Estimation through Migration

Radar file before (left) and after (right) migration. The slope of the limbs of the diffraction hyperbola (gray curve at left) is a function of the soil velocity. The use of the correct migration velocity redistributes diffracted energy back to a single point (circled on the right panel), whereas incorrect velocities result in over- or under-migrated energy.

Elevation Correction: Topographic corrections were applied to records recorded for transverse profiles (down the embankment slope). The purpose of the correction is to return the features observed in the radar record to their correct geometry (Figure 5). Measured topographic elevations at all grid intersection points were correlated with location markers in the radar records. The radar data were used to the measured elevations at the markers and interpolated elevations between the markers. After the elevation correction, some reflectors that were originally sloping are rotated into a near-horizontal orientation.

Above Ground Reflection: An apparent reflection from power lines was present in the transverse profiles. Although the dipping reflection could have been removed from the data using f-k (frequency-wavenumber) filtering, the method imparted significant noise into the data and degraded the record more than the presence of the above ground reflection. The above ground reflection was easily identified in the data and occurred later in the record than most features of interest. Consequently, the reflection did not significantly affect interpretation efforts, and was not removed except for specific evaluations.

Three Dimensional Data Volume: To assist in the interpretation of the dam as a whole, 52 transverse profiles were compiled into a three-dimensional data volume. This allowed the visualization of all transverse radar data across the entire dam surface, and allowed reflections that appear relatively incoherent in individual records to be correlated over many parallel profiles.

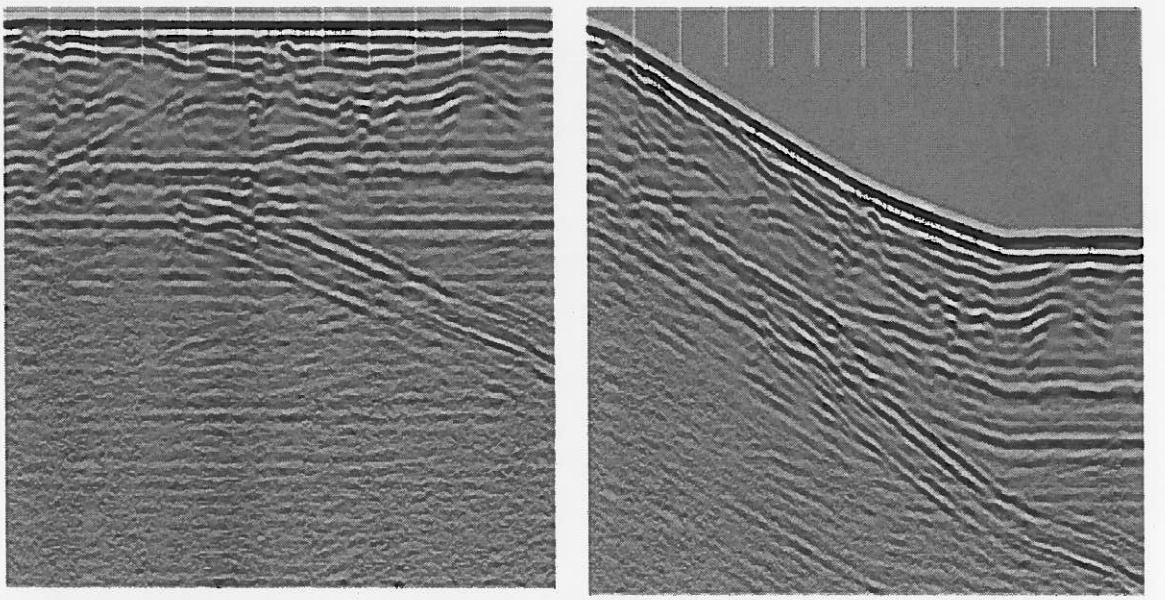

Figure 5. Elevation Correction

Radar file before (left) and after (right) elevation correction. Note that some once dipping features become nearly horizontal.

DATA INTERPRETATION

Above Ground Reflection

Radar records from the transverse profiles contain a prominent band of reflections that dips in the down-slope direction. This band of reflections is apparent during all stages of processing, as evidenced in the lower half of the records depicted in Figures 2, 3 and 5. Analytical modeling of arrival times versus antenna offset distances indicates that the reflections are from the overhead power lines at the crest of the dam even though a shielded antenna was used for the survey. Figure 6 shows a typical record for a transverse profile before any data processing was applied. Although a shielded radar antenna was employed, the correlation between the calculated and the observed reflections offers compelling evidence that radar energy was reflected from overhead objects.

Interpreted Phreatic Surface

With a few exceptions, continuous and coherent reflections were not recorded from the top of the phreatic surface. Phreatic surface reflections are often poorly developed because of the occurrence of fine sediment in the embankment soil. Continuous and coherent reflections from the phreatic surface are more frequently observed in coarse sediments with comparatively large, open pore spaces, such as coarse sand and gravel. Capillary pressures in fine pore spaces result in a gradual increase in saturation (a wider capillary band), not a sharp saturation margin. Consequently, propagating radar energy does encounter a sharp reflecting boundary and phreatic surface reflections typically are not well defined.

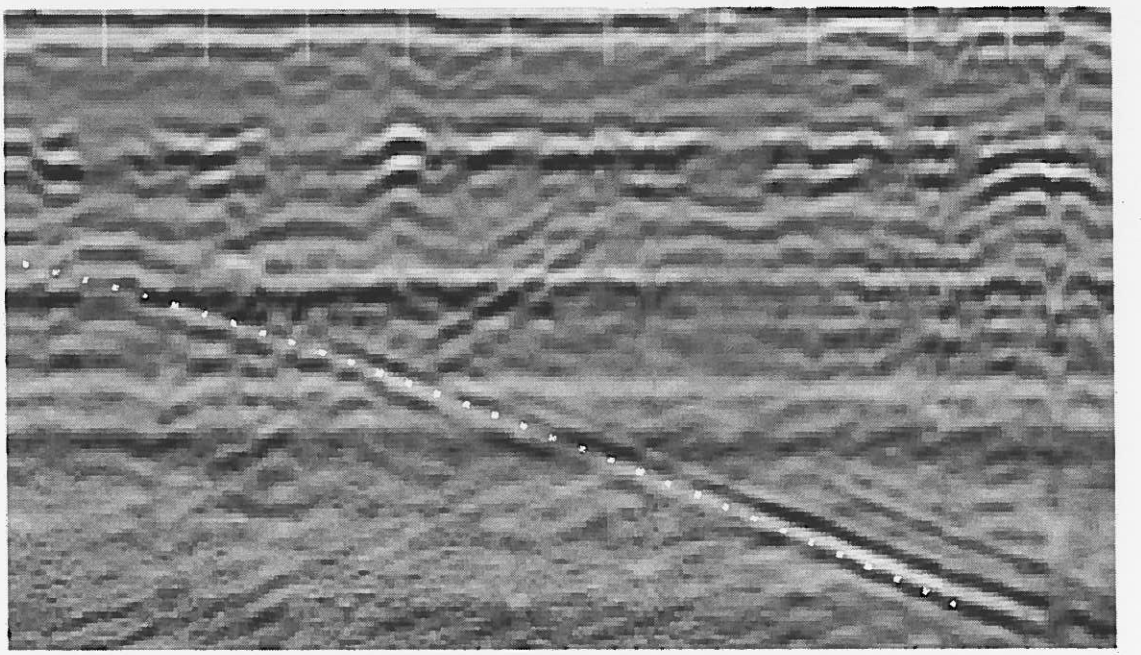

Figure 6. Power Line Reflection

Radar file before elevation correction showing reflections interpreted as power lines. Image is typical for all transverse profiles. Dotted white line shows calculated reflection arrival time with offset (scaled to radar image). Although a shielded radar antenna was employed, the correlation between the calculated and the observed reflections offers compelling evidence that radar energy was reflected from overhead objects.

However, there were some records where a good reflection was interpreted to represent the top of the first saturated zone. (Note that the phrase Étop of first saturationÊ is used because the shallowest saturated zone may represent perched ground water, not the top of the phreatic zone or ground water table.) As discussed, the presence of water in saturated soil results in an increased dielectric coefficient for the soil, and the boundary between the saturated and overlying soil can produce high amplitude reflections. Figure 7 shows a well-defined reflection that is interpreted as the ground water surface for a record collected approximately 20 ft south of the embankment wall. (The power line reflections were removed from this profile using f-k filtering, which improved the continuity of the groundwater reflection in the upslope portions of the embankment.)

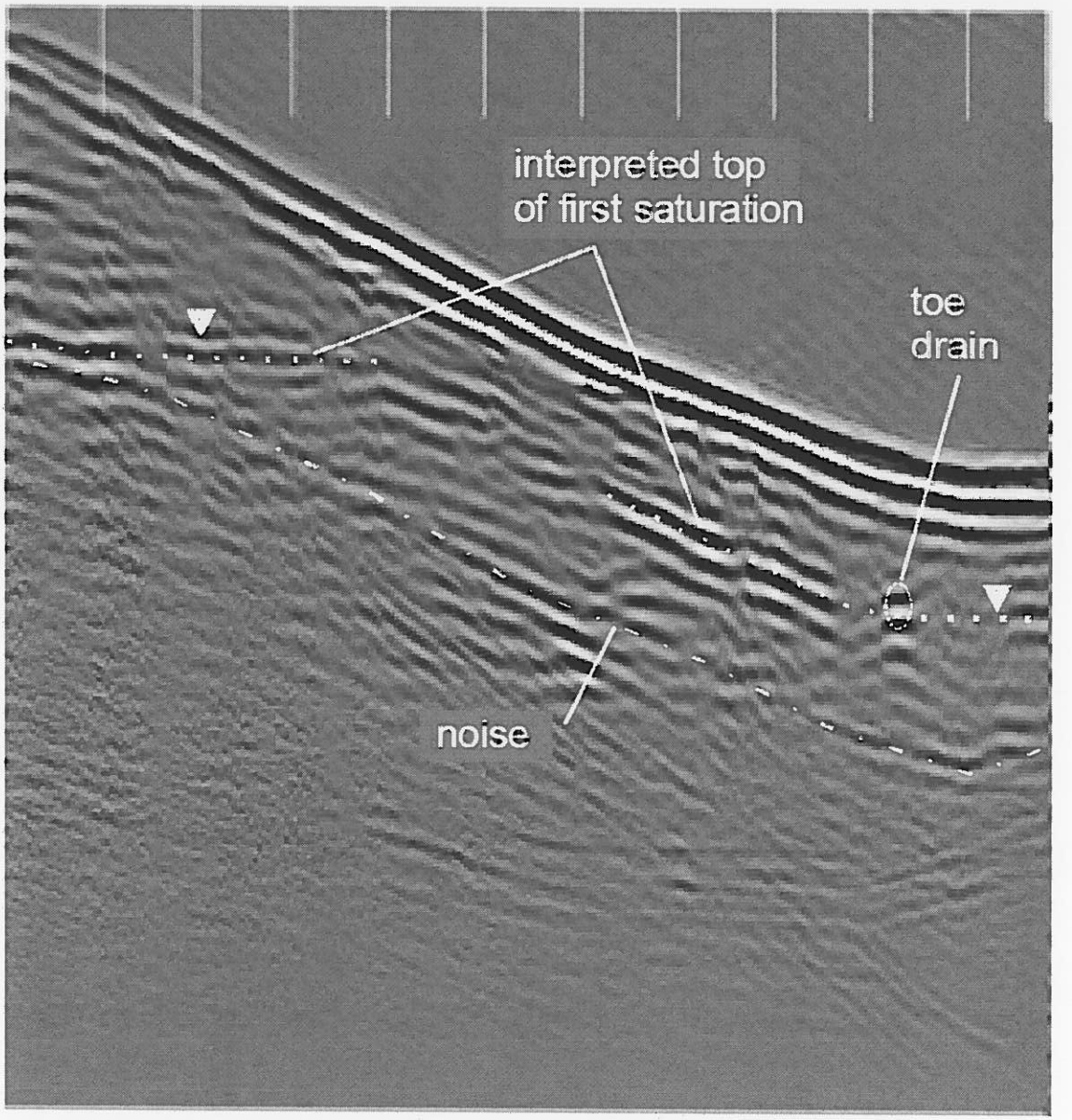

Figure 7. Interpreted Top of Saturation within Seepage Area

Radar profile showing reflection interpreted as the top the first saturated unit. Dotted line marked with triangles shows interpreted top of saturated zone. Line to right (down-slope) may represent a lateral drain (see Figure 13). The underlying dashed line, while appearing schematically as a possible groundwater reflection, is a type of noise shown more prominently in Figures 2 and 3. Toe drain is represented as high amplitude anomaly.

Figure 8 is a radar profile collected near the seepage zone. The image has been rescaled to match that of a schematic drawing showing historical water levels within five piezometers (P-1, P-3, P-5, P-8 and P-13). This figure shows a good correlation between the interpreted groundwater reflections and the known piezometer levels. It should be noted that the radar image was linearly stretched to match the scale of the drawing but the scales of the two are not the same; the vertical scale dimensions are time for the radar image and distance for the drawing. Figure 9 is the same radar record. The antenna was pulled sequentially within a few feet of several piezometers. A near-horizontal reflection is interpreted as a zone of perched water midway down the

embankment slope. This interpretation is supported by the proximity of the point of intersection of the reflector and the embankment surface with the observed seepage near a piezometer. The interpreted perched groundwater reflection is present in other data records within a zone from 75 to 105 ft south of concrete abutment and is less well defined or apparently absent on others (see Figure 8). An alternative but seemingly less likely interpretation is that the flat reflector is due to a preexisting bench created during the period when modifications were made.

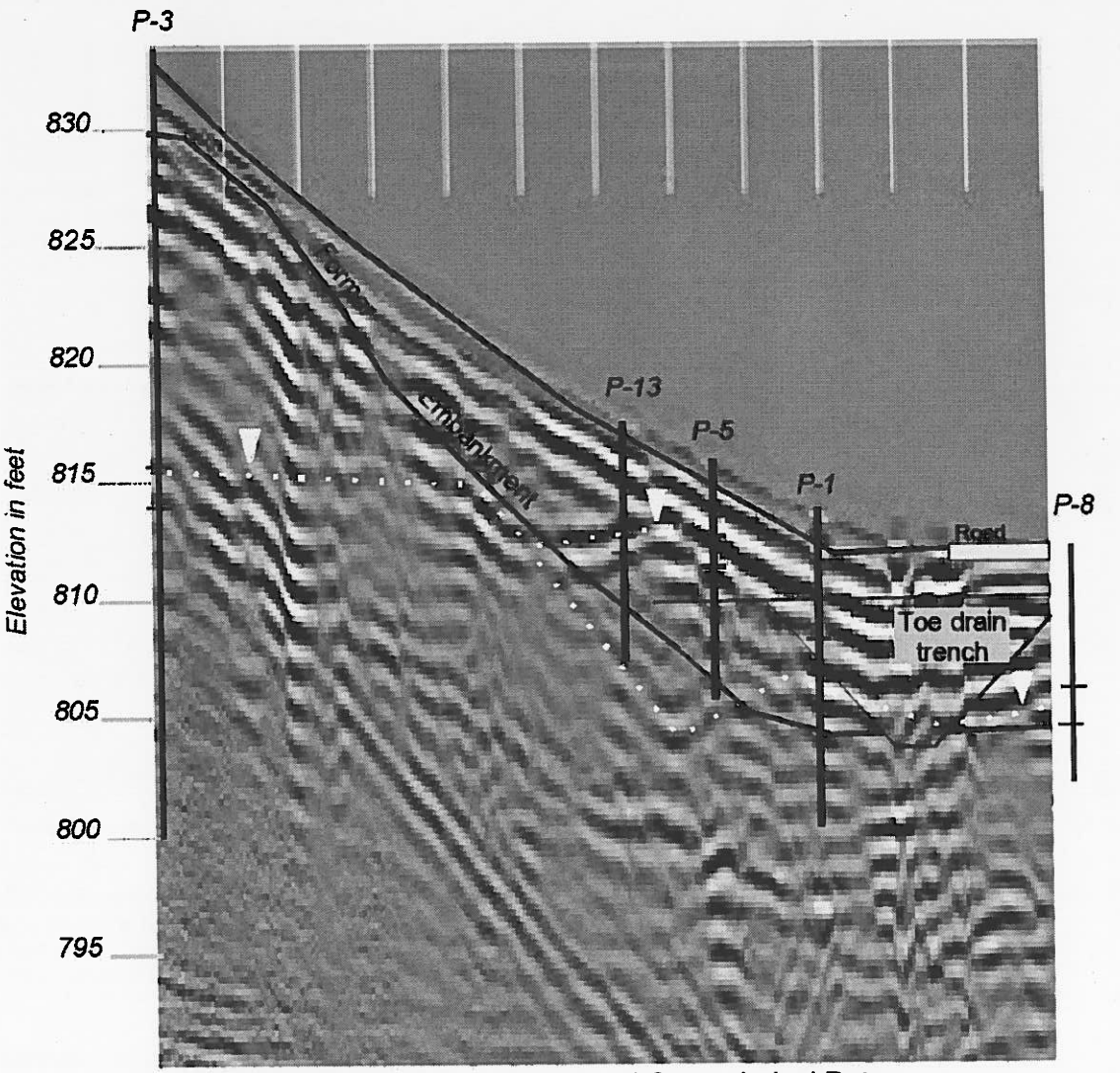

Figure 8. Integration of Radar and Geotechnical Data

Transverse radar profile with geotechnical data overlay. Note that the vertical dimension is time for the radar data and depth for the schematic drawing. Nevertheless, there is a good correlation of interpreted groundwater reflections (dotted line annotated with triangles) and historical ranges of water levels (shown as fine horizontal ticks) in the piezometers. The toe drain cannot be discerned in this image.

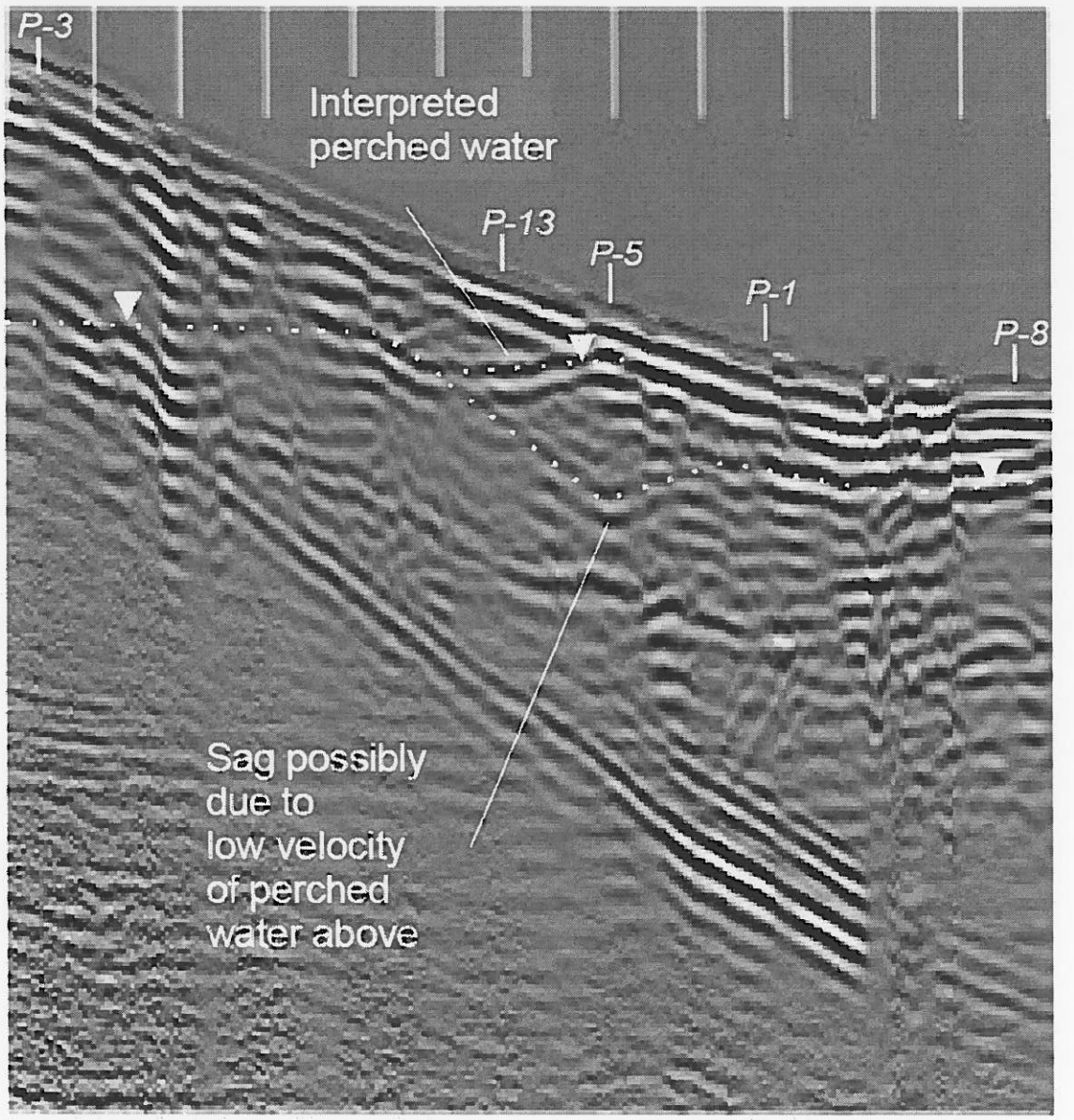

Figure 9. Interpreted Perched Water at Seepage Area

Radar profile near the observed seep zone (90 ft south of abutment). Dotted line marked with triangles shows interpreted top of phreatic zone. The dip beneath the interpreted perched water is possibly due to the lower velocity of the overlying saturated zone. The deeper planar dipping reflections are due to overhead power lines as discussed.

A significant snow cover was in the process of melting during the period of the radar survey. The effect of the meltwater on the data sets has not been extensively analyzed, but it was assumed to cause trivial ground water mounding. The wet surface soil conditions would generally result in increased resolution but decreased depths of penetration. Meltwater seeping into the units could also result in accentuation of soil boundaries with only subtle physical differences. Figure 9 also shows the presence of high amplitude reflections (high amplitudes are represented as white or black opposed to a shade of gray) near the ground surface that are possibly a combination of seep water and snow melt.

Evaluation of Possible Void Occurrence

A void within the dam is considered an area where soil or fill has been removed; leaving a cavity filled with either air (in the unsaturated zone) or ground water (in the saturated zone). The radar anomaly resulting from such a void would be characterized by the presence of high amplitude, ringing waveforms (recognized in radar records as vertical bands of reverberating energy). Because the radar profiles were spaced at 3-ft intervals, an anomaly appearing on only one profile could be of a significant (3+ ft) dimension, but uncorroborated by a similar anomaly on an adjacent profile.

A sketch was provided documenting the location of grout injection points in the south abutment wall. The transverse radar profile nearest the abutment was processed (by f-k filtering) to mute reflections oriented parallel to the ground surface so that subtle, discontinuous anomalies are accentuated. The resulting profile (Figure 10) contains nine small anomalies that correspond (within one ft of accuracy) with the lateral locations of the grout injection points presented mentioned sketch. A high-amplitude anomaly that extends down-slope approximately 6 ft is interpreted as a suspect void, representing an area that grout did not reach. The suspected void is estimated to be 8 ft beneath the surface at a point 36 ft down the embankment slope (west of a surface monument). Individual radar profiles and the three-dimensional data volumes created from transverse and longitudinal profiles revealed many anomalies that have characteristics that are generically similar to those expected from voids (high amplitude ringing waveforms). Many of these anomalies are clearly associated with known and identifiable features, but their presence clutters the data and reduces the ability to isolate a group of anomalies that match the stated criteria. Table 1 presents thirteen locations where radar anomalies exhibit the stated criteria, and cannot be attributed to other known features. All of the listed anomalies are relatively small in extent (a few feet) and are scatted apart from one another, suggesting that extensive and continuous voids are not present up to the depth of the survey (approximately 10 to 15 ft).

Table 1: Summary of Anomalies Consistent with the Presence of Voids

Anomaly	Southing[1]	Westing[1]	Depth[2]
1	0	32	8
2	3	35	6
3	6	43	6
4	24	22	6
5	30	11	4
6	39	40	6
7	39	50	6
8	50	28	6
9	95	30	5
10	99	23	7
11	144	39	6
12	150	44	6
13	144	50	6

1 Å distances indicated are ft south and west of a surface monument
2 Å depth in ft assuming the dielectric constant = 9

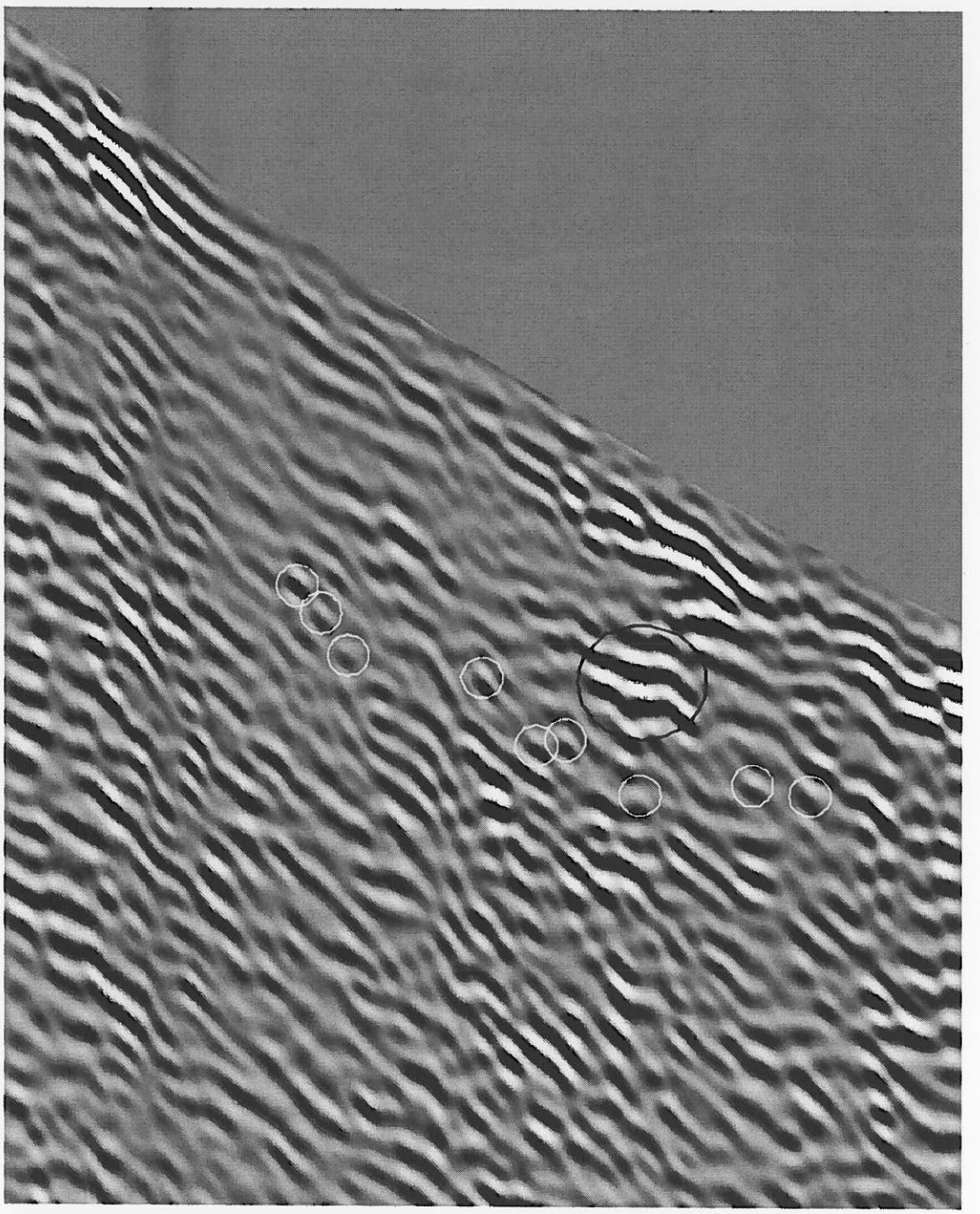

Figure 10. GPR Image of Grout Injection Zone

Radar profile nearest the south embankment wall. Light gray circles identify anomalies that correlate (within 1 ft. of accuracy) with the location of grout injection locations. The large dark circle indicates an anomaly suspected to be a void. The depth of the void is estimated (assuming the dielectric constant $\varepsilon = 9$) to be approximately 8 ft beneath the surface at its midpoint.

Toe Drain

The toe drain was successfully imaged in only 9 of 52 transverse profiles, and was not well defined on the longitudinal profiles. It is not known why the toe drain is

sporadically imaged in the transverse sections, but the generally wet soil conditions at the base of the embankment likely contributed to the poor radar image quality. The longitudinal profiles, oriented parallel to the toe drain, suggested the presence of saturated intervals (high amplitude reflections) along the length of the trench, but did not reveal much about the structure of the drain. Figure 11 is an interpreted image of the toe drain and the interpreted top of first saturation from a transverse profile. High amplitude reflections observed within the trench are interpreted as accumulated water in the pipe or trench.

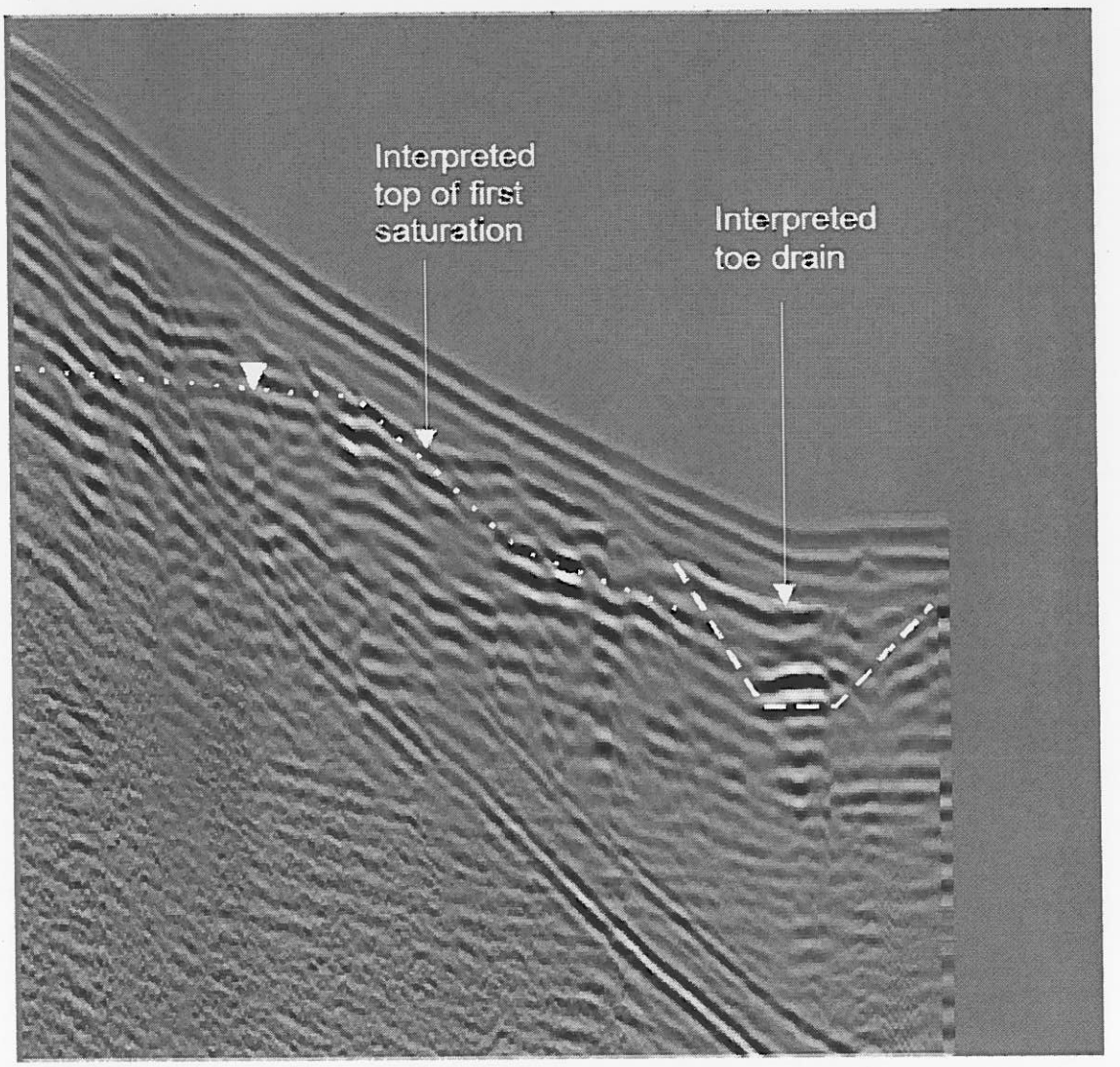

Figure 11. Imaged Toe Drain

Radar profile where toe drain is well imaged (132 ft south of surface monument). The high amplitude reflection at the base of the drain is interpreted to represent collected water within the trench or drain pipe. The interpreted zone of first saturation is consistent with interpretations elsewhere on the embankment. Note the abrupt discontinuation of phreatic surface at toe drain trench.

Lateral Drains

Lateral drains were detected in six of the longitudinal profiles that were located from 29 to 43 ft west (in the down slope direction) from the crest of the dam. Evidence of the drains was generally absent in profiles recorded higher up the embankment, which is a likely result of the increasing overburden thickness. In the longitudinal profiles, the drain anomalies consisted of poorly- to well-defined hyperbolas that generally correlated with the approximate locations of laterals as determined in a video inspection of the toe drain. No apparent correlation exists between the nature and occurrence of the radar anomalies and the flow rate reported for the lateral drains (Figure 12). Lateral drains also appeared to be imaged in a few transverse profiles that happened to directly overlie the lateral drains (Figure 13). In these cases, high amplitude anomalies were present at the point the drain crosses through the interpreted former embankment surface extending to the point the lateral enters the toe drain.

CONCLUSIONS

1. The phreatic surface could not be clearly identified in all of the radar records. Although the saturation boundary could be identified in several profiles, it was often a discontinuous and incoherent reflection. However, a consistent surface was apparent over a series of profiles, and with good correlation with historic water level measurements (Figure 8).

2. There is evidence that perched water is present in the embankment seepage area. Radar files collected in the downslope direction near Piezometer P-5 exhibit a faint horizontal reflection interpreted as perched water (Figure 9). Similar horizontal reflections were observed in files collected from 75 to 105 ft south of the surface monument. There was no apparent mechanism for the localization of perched water.

3. A suspected void was identified near the grouted south abutment wall. The radar survey appeared to image several of the grout injection points, and is 8 ft deep, 6 ft wide (in the down-slope dimension) and is located approximately 36 ft down the embankment slope.

4. Radar anomalies were present that are consistent with scattered small voids, but large continuous voids are apparently absent. Assuming a void would be characterized by high-amplitude ringing waveforms, several anomalies were identified that both exhibited this criteria and were could not be attributed to known features (Table 1). All of the identified anomalies are relatively small in extent (a few feet) and are scatted relative to one another. No anomalies consistent with the presence of large, laterally extensive voids were observed to the depth achieved by the survey (approximately 10 to 15 ft).

5. The locations of the toe and lateral drains could be imaged by radar, but no information about their function could be determined. Radar images of the toe and lateral drains (Figures 9, 10 and 11) allowed the identification of the drains. However, no information was gleaned about the mechanisms and processes affecting the drains. There was no apparent relationship between the drain anomalies and their reported flow rates.

6. A grouting program was undertaken according to the information presented in Table 1, and little information was recorded regarding grout takes.

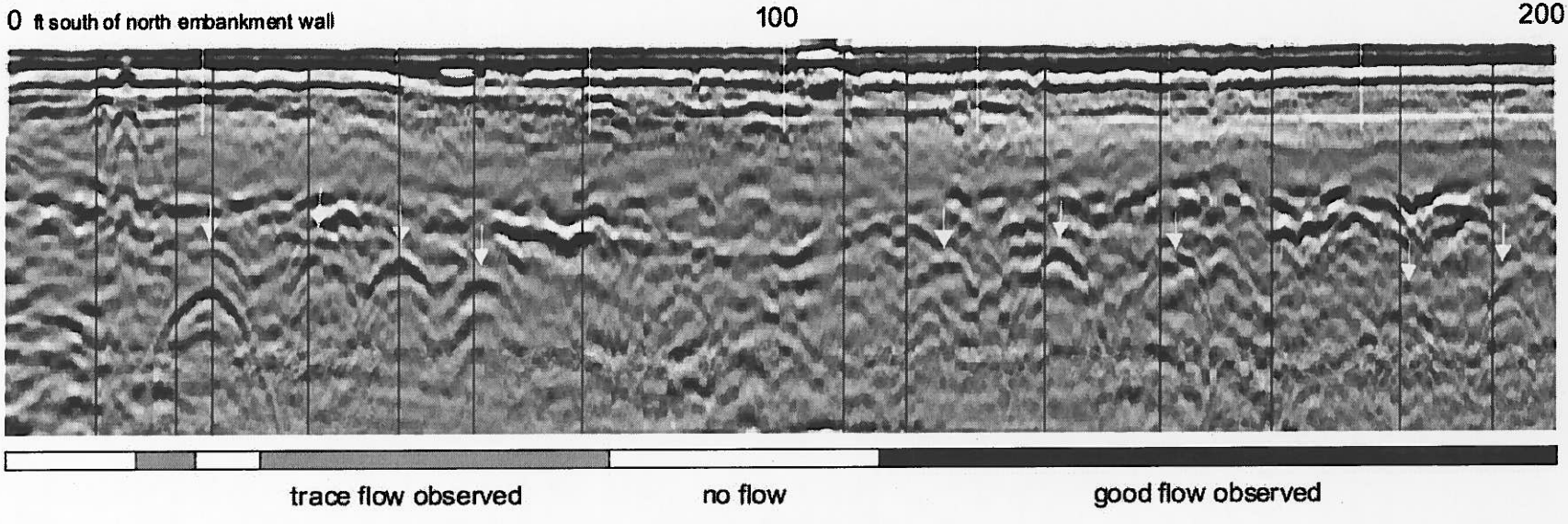

Figure 12. Lateral Drains Imaged in Longitudinal Profiles

Longitudinal radar profile showing interpreted toe drains as broad diffraction hyperbolas. The tops of the hyperbolas are marked with light gray arrows and the lateral drains are represented by black vertical lines. The scale bar at bottom indicates the reported flow through the drains at the time of a video inspection with good flow shown in black, trace flow in gray and no flow conditions in white.

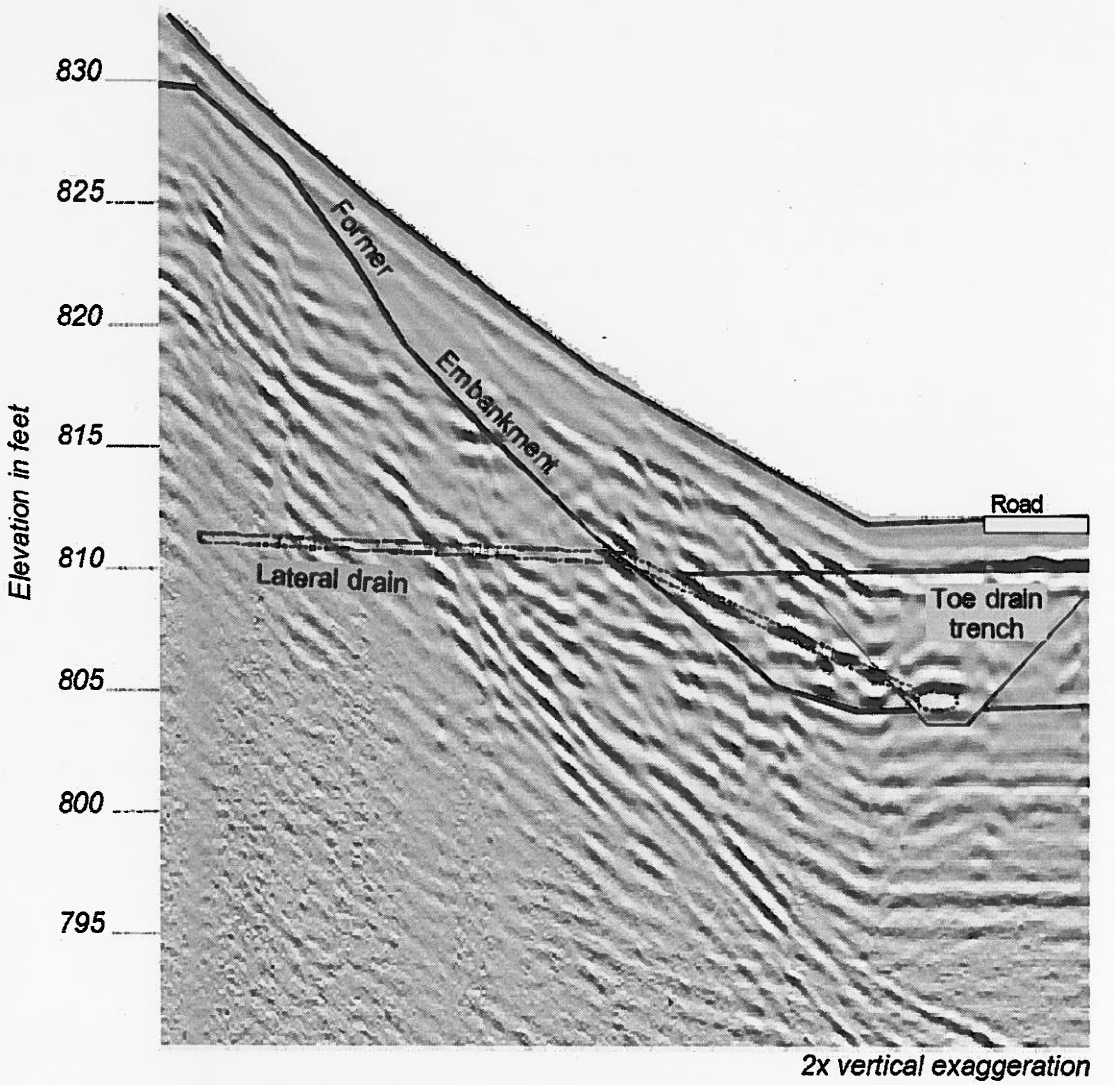

Figure 13. Lateral Drain Imaged in Transverse Profile

Transverse radar profile showing high amplitude (white and black) anomalies that correlate with the location of the lateral drain provided in an engineering drawing. Note the abrupt increase in the drain anomaly when it crosses the former embankment surface and when it enters the toe drain trench.

REFERENCES

Farrand, W.R. and Eschman, D.F. (1974). ÉGlaciation of the southern peninsula of Michigan.ÊMichigan Academician Vol. 7, 31-56.

Lineback, J.A., Blever, N.K., Mickelson, D.M., Farrand, W.R., and Goldthwait, R.P. (1983). Quaternary Geologic Map of the Chicago Quadrangle, United States Department of the Interior, Geological Survey, Washington, DC.

DGI-MENARD, Inc.
Ground Improvement Specialists
Sustainable Technology

Controlled Modulus Columns™ (CMC) for Support of Above-Ground Storage Tanks

Prepared for:
Ohio River Valley Soils Seminar XL (ORVSS)

Date:
November 13, 2009

Author:
Frederic Masse, Vice President of Engineering
fmasse@dgi-menard.com
ASCE, GI, DFI, CAWP

Seth L. Pearlman, P.E., President and CEO
spearlman@dgi-menard.com
ASCE, GI, D.GE, DFI, MOLES, DBIA, ACI

Martin G. Taube, P.E, P.G., Director of Business Development
mtaube@dgi-menard.com
ASCE, GI, DFI

DGI-Menard, Inc.
275 Millers Run Road
Bridgeville, PA, 15017
Phone: (412) 257-2750
Fax: (412) 257-8455

Word count: 5,046

ABSTRACT

Controlled Modulus Columns™ (CMC) are pressure grouted auger displacement elements that are installed using a specially designed tool at the working end of a high torque, high down-pressure drilling machine. The tool is hollow so that flowable cementitious grout can be placed from the bottom up once the tool is advanced to the desired depth. The patented CMC system fits in the generic category of inclusions. There are a number of other types of inclusions that are currently designed and constructed using stone, grout, and concrete. The design technology and experience with CMC makes them uniquely efficient for the immediate support of large liquid or bulk solid storage tanks, as well as MSE walls and embankments for public transportation, other infrastructure facilities, buildings, and other structures.

Large-diameter, above-ground storage tanks impart heavy loads, deep into the ground, extending over a wide area. In many locations, the ground is stiff enough to safely support tanks without excessive settlement. However, many terminals, refineries and storage facilities are located along waterways and coastal plains in areas with soft compressible ground, or on uncontrolled fill that cannot safely support tanks. The support options in these areas have traditionally included: removing and replacing the existing soft ground; or installing deep foundation systems, such as piles with a concrete mat to support the tank.

CMCs are an ideal solution for the immediate support of large storage tanks. Using specialized drilling rigs, control of bearing layer penetration is provided in a consistent fashion, and electronic monitoring and recordation of drilling and grouting parameters is routinely used for quality control. The load is distributed to the CMC elements using a compacted granular load transfer platform that serves as an efficient and cost effective foundation. Other features such as leak detection and cathodic protection are detailed into the load transfer platform.

CMCs are designed using special proprietary finite element techniques that include the effects of load sharing between the distribution mat, the columns, and the surrounding improved ground. Special considerations for bearing into the distribution layer are made, as well as detailed designs for interaction with concrete or granular ring walls.

INTRODUCTION

Some amount of settlement occurs when any tank is built and put into service. The settlement is only problematic when it exceeds the tolerance for the tank or lines connected to the tank. The amount that a tank will settle is dependent on the tank loading properties (i.e., the diameter and the weight of the tank and its contents) and the soil properties (both elastic stiffness and long term settlement parameters) of the underlying soils. The settlement for similarly sized tanks at different locations may vary from an inch or less to 10 feet or more, depending on the range of ground conditions at the different locations. The amount that an individual tank settles is not always uniform for the entire tank as the substrata may vary significantly beneath the tank footprint. The tolerance that tanks have for differential settlement is significantly less than the tolerance for the maximum uniform settlement that can be withstood, with tanks that have floating roofs being the most sensitive to settlement.

In addition to excessive settlement, bearing capacity failure may occur where weak soils are present. This occurs when the underlying soils cannot carry the load from the tank and the ground shears or ruptures, causing either a rotation of the tank or punching of the tank into the ground. Although bearing capacity problems are less common than settlement problems, when bearing capacity failures occur, they are typically catastrophic in terms of the performance and servicability of the tank, with a very high risk of tank rupture and significant product loss. Failures occur when the weight of the tank induces stresses into the ground that the underlying soils are too weak to handle. Bearing capacity failures are rare, but when they do occur, may occur rapidly.

GROUND IMPROVEMENT FOR TANKS

Where weak soils are present in areas where tanks are to be built and it is not practical to change the location of the tanks, the weak ground can be replaced, bypassed with piles, or treated by a number of different ground improvement technologies. Removing and replacing soft ground with compacted backfill can be impractical or very costly when the soft ground extends below a few feet or if it is necessary to excavate below the groundwater table. At sites with very weak near-surface soils, the ground cannot safely support the construction equipment that is needed to excavate and haul away the soft soils. Installing piles to transfer the load from the tank to underlying bearing layers can be costly, and typically requires that a thick, heavily reinforced concrete mat be constructed to form a monolithic slab upon which the tank is founded. At some sites, the ground can be improved adequately just by surcharging the tank footprint (with a temporary pile of soil or by filling the constructed tank with water), and letting the weight of the surcharge consolidate the underlying soils. However, the surcharge process (in the absence of wick drains/prefabricated vertical drains) can take years or decades where the soils are slow draining.

For tanks, the goals of ground improvement are to reduce the total and differential settlement that occurs while tanks are in service, to increase the factor of safety against bearing capacity failure, and at some locales to reduce the risk that the soils supporting a tank liquefy during seismic events (i.e., earthquakes).

CONTROLLED MODULUS COLUMNS (CMCs)

Deep foundations are rigid structural elements that are used to transfer the load from the structure to competent layers below (bedrock, dense or stiff soils) by "bridging" the compressible soft soils. Because the loads are highly concentrated on the elements, the elements need to have direct contact with the structure to be able to transmit these loads either through end-bearing, skin-friction, or a combination of the two. Deep foundation systems are designed to allow minimal settlement and when used to support tanks, they require the use of a structural mat, or pile cap to connect the tops of the piles together to provide a foundation for the tank. The structural mats add significant costs to the project.

While more "deformable" ground improvement solutions (e.g., stone columns or aggregate piers) are often very economical compared to a deep foundation system, the expected and observed settlements are typically greater than that of rigid deep foundations. In the case of stone columns for example, the ratio of stiffness between the soil and the stone column determines the ratio of load shared between the soil and the element. Settlement is a factor of the stress carried by the stone columns and the soil and the respective compressibility of column material and the surrounding soil. Stone column design is based on the assumption that the column and the surrounding soil are compressed, or settle, equal amounts. When ground improvement is used, the load concentration in each element is significantly reduced as compared to a deep foundation system, and the structure need not be as rigid. With ground improvement, structures can be designed as if it they are founded on competent ground with a slab-on-grade and spread and strip footings, or in the case of storage tanks, using welded bottom plates and a peripheral ring wall without the need for a pile cap/mat beneath the tank.

Controlled Modulus Column™ (CMC) technology bridges the gap between these two different approaches (deep foundations and deformable inclusions) by reducing the global deformability of a soil mass using semi-rigid soil reinforcement columns. The soil–CMC mass behaves as a composite mass of greater stiffness than the initial untreated ground, reducing settlements induced by the weight of the structure to within allowable ranges. CMCs are not intended to directly support the loads imposed by the structure, but to improve the global response of the soil in order to control settlement. The dimensions, spacing, and composition of the CMCs are based upon the development of an optimal combination of support from the columns and the surrounding soil to limit settlements for the project within the allowable range, and to obtain the required value for the equivalent composite deformation modulus of the improved soil.

Some features of the CMC technology include:

- Material is grouted in place with the use of a displacement auger in order to reinforce the ground
- Deformation modulus of the CMC elements is 50 – 3,000 times that of the soil (weakest stratum)
- A load transfer platform of generally granular fill (LTP) is placed over the CMC reinforced ground that has a modulus less than that of the CMC elements which can be partially penetrated by the inclusions to promote strain compatibility/ load sharing between all the components
- In granular soils, densification due to the lateral displacement may occur between the columns by virtue of the displacement drilling process
- Virtually no spoils are generated by the drilling process which eliminates the need to manage spoils and the potential unearthing of contaminated soils

The tops of CMCs are typically installed 1 to 3 feet below the bottoms of the shallow foundations. A layer of compacted granular material referred to as the load transfer platform (LTP) is installed above the top of the CMCs and below the structure following installation of the CMCs. The main purpose of the LTP is to transfer the load from the structure to the CMCs without using pile caps between the structure bottom and the CMCs. The load is transferred to the CMCs through arching within the high phi-angle LTP and through side friction below the top of the CMCs. The system is generally designed to transfer 50 to 95% of the load to the CMCs while the remainder of the load is transmitted to the soils between the CMCs. The ratio of load sharing is dependent upon the type and stiffness of the soils between the CMCs as well as the allowable settlement for the structure.

The CMC technology is very well suited for very soft soil conditions such as organic clays, peat and wastes. Compared to stone columns that require a significant degree of lateral confinement to avoid bulging when loaded, CMCs have no such limitations due to the relatively high stiffness of the column material.

The installation of CMCs does not generate vibrations so the technology is ideally suited for construction in urban areas (working close to sensitive structures). CMCs are commonly used to support structures such as storage tanks, buildings, warehouses, industrial facilities, culverts and pipes, as well as platforms, embankments, retaining walls, and bridge abutments. The CMC columns typically range from 12 to 18 inches in diameter.

Installation of CMCs

CMCs are installed using a specially designed displacement auger that displaces the soil laterally without generating spoils or creating vibrations. The displacement auger is hollow, which allows for continuous placement of the grout as the auger is withdrawn. The grout for the CMC element is placed with enough back pressure to avoid collapse of the displaced soils during auger withdrawal (typically the static head of grout plus less than 100 psi is necessary). The installation process allows for the creation of a column with the diameter that is at least as large as that of the auger. CMCs are installed with drilling equipment that has large torque capacity and high static down thrust.

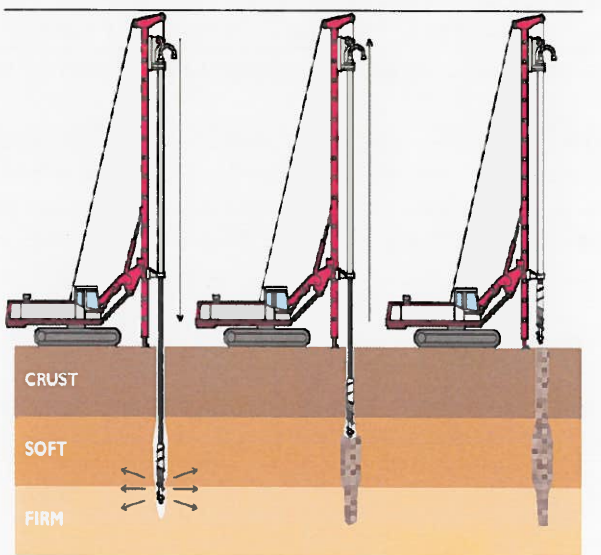

FIGURE 1 CMC installation schematic.

Upon reaching the desired depth, grout is pumped through the hollow stem of the auger and into the soil bore as the auger is withdrawn at a pre-defined rate that is calibrated to avoid necking.

With a conventional continuous flight auger, "negative displacement", stress relief, or even lateral mining around the auger is inevitable. This creates a movement of the surrounding soils which are loosened by the augering process toward an active (Ka) condition. This condition creates a risk of necking. On the contrary, with the CMC displacement auger, the effect is opposite: the soil adjacent to the auger is displaced laterally by the displacement stem portion of the auger and brought to a denser passive (Kp) state of stresses. Stress relief does not occur and the risks of necking the CMC are quasi-inexistent, except with operator error.

Quality control of the CMC and monitoring to catch any operator error is done with real time monitoring of the following installation parameters:

- Speed of rotation
- Rate of advancement and withdrawal of the auger
- Torque, down-thrust (crowd) during the drilling phase
- Depth of element
- Time of installation
- Grout pressure in the line at the top of the drill string
- Volume of grout as a function of depth

The grout pressure is monitored by a sensor located at the top of the concrete line above the swivel attached to the mast drilling head. The CMCs are usually installed using a target overbreak of 5 to 10% of the volume of grout. During the grout phase, pressure readings are kept to a moderate positive pressure. Any loss in pressure can reveal a soft or loose soil zone that may not have been detected during the geotechnical investigation.

A significant benefit of the recordation of installation parameters is that changes in subsurface conditions can be detected in the field, and more importantly, column depths can be adjusted based on the encountered conditions as detected by the response of the drilling equipment. The recorded drilling parameters of down pressure, speed and torque are readily interpreted in the field during drilling and changes in stratigraphy can be sensed based on ease or difficulty of drilling. This ability to adjust column lengths in the field offers a significant advantage over most other forms of column installation.

Other forms of QC include monitoring fluid grout properties for consistency with the expectations of the design mix, and sampling, curing and testing of samples for grout strength. Load testing (ASTM D1143) is routinely done when there is no previous experience with elements capacities in the subject strata. Other in-situ testing such as PIT (Pile Integrity Tests) and dynamic loads tests (e.g. Statnamic) have also been used.

The CMC Design Concept

The behavior of an individual inclusion is predicated on reaching equilibrium under loads (Combarieu, 1988) as shown on Figure 2. While the inclusion is being compressed by the load, negative skin friction is acting in its upper part and positive skin friction in its lower part. When the equilibrium is reached, the stresses acting on the inclusion can be divided into four components:

- The vertical load, Q at the top of the inclusion
- The negative skin friction acting on the upper portion of the inclusion
- The positive skin friction acting at the lower portion
- The vertical reaction at the tip

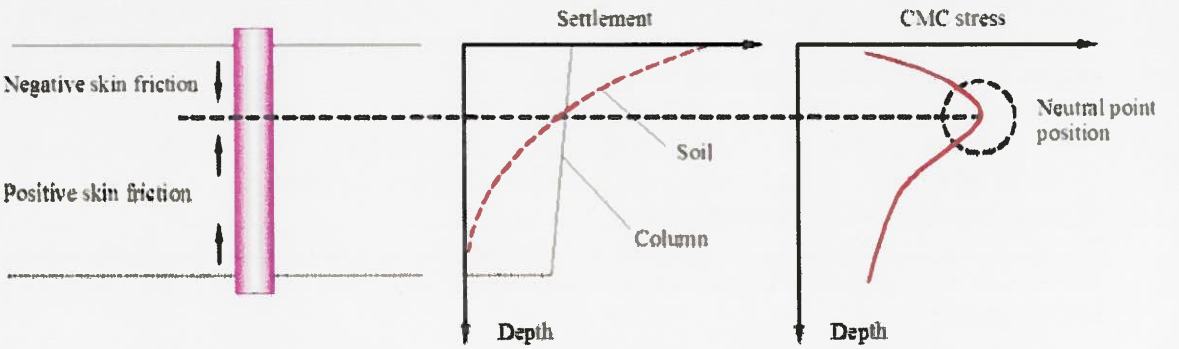

FIGURE 2 Settlement distribution between soil and an isolated inclusion.

The load of the structure is usually distributed to a network of inclusions by the LTP. Figure 3 shows how the load is distributed from the structure to the bearing layer. The load distribution between CMCs and surrounding soil is based on reaching an equilibrium between deformations of the CMCs and the surrounding soils. The design of a network of inclusions is thus based on a good knowledge of the distribution of stresses and deformations in the soil and the inclusions.

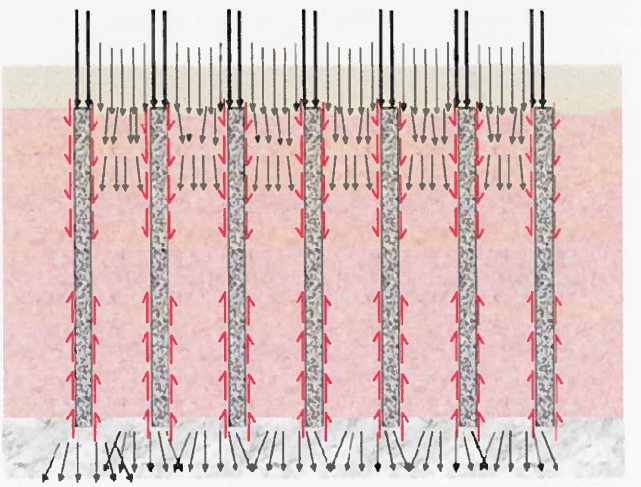

FIGURE 3 Load distribution between soil and an inclusion network.

While calculation methods have been proposed by various authors (see Combarieu), with the development of more powerful computers, finite element method (FEM) analysis has quickly become the method of choice when designing a network of CMCs.

CMCs FOR STORAGE TANKS

CMCs have been used to support numerous bulk liquid and solid storage tanks around the world. Some of the factors why CMCs are so commonly used for support of storage tanks include:

- Many refineries, terminals and industrial facilities are located in coastal areas or along waterways where very soft alluvial soils are present;
- Storage tanks with denser product or greater product heights may exert extremely high bearing pressures that renders ground improvement solutions using deformable inclusions inadequate due to excessive settlement or bearing capacity failure;

- Because of the very deep zone of influence of large storage tanks, in areas it is necessary to extend the CMCs to depths of 100 feet or deeper. Achieving such depths with many other forms of ground improvement is typically not practical;
- The heavily reinforced concrete pile cap required if piles are used is not necessary;
- Many tanks are constructed where contaminated ground is present. Only a negligible amount of spoils are generated. These materials are readily worked into the platform and disposal/management is not required; and,
- Because CMCs are sealed by virtue of the grouting process and self cased drilling, aquacludes are not breached and potential migration paths for contaminated groundwater or leaked product are not introduced.

CMCs are typically installed 1 to 3 feet below the tank bottom. A compacted granular LTP is installed above the top of the CMCs and below the tank after installation of the CMCs. The main purpose of the LTP is to transfer the load from the tank to the CMCs without the use of pile caps between the tank bottom and the CMCs. The load is transferred to the CMCs through arching within the high phi-angle LTP and through side friction below the top of the CMCs. Because the CMCs are totally isolated from the structure, utilities, vapor barriers, cathodic protection systems, and liners can be easily installed directly under the tank bottom within the LTP.

CMCs are usually installed beneath the centerline of the concrete ringwall that supports the tank shell. The CMCs typically terminate 6 to 12 inches below the bottom of the wall. The spacing of the elements below the ringwall is governed by the ability of the surrounding soils to share the load with the CMC elements while maintaining deformations within acceptable tolerances. The LTP is typically extended beneath the ringwall and occupies the zone between the top of the CMC columns and the ringwall. In effect, the LTP may be thought of as a cushion that separates the tank and ringwall bottom from the top o the CMCs.

CMCs may be designed to accommodate moderate uplift conditions by placing a centralized bar in the elements and extending the bar into the ringwall as required. This is sometimes required where tanks are situated in flood prone areas.

CASE HISTORY - PETROLEUM STORAGE TANK, PORT OF QUEBEC CITY, QUEBEC

This project involved the improvement of the foundation soils for five petroleum product tanks at a facility in the Port of Quebec City. The 120 foot diameter tanks were planned to be built on a structural slab supported by a network of pressure injected footing type piles.

To reduce construction costs, a ground improvement solution using CMCs was proposed. The requirement for the ground improvement was to achieve a net bearing capacity of 5 kips/sf. The computed post-construction differential settlement was required to be less than 1 inch, which corresponds to an angular deflection of 1:730.

Geotechnical Conditions

Stratigraphy over the site of the five tanks was typically composed of a loose surficial fill of silty sand varying to sandy silt about 16 feet thick, covering a layer of wood and organic waste material with lenses of silt and sand. The total thickness of the organic layer varied between 5 and 8 feet. Natural dense sand with some silt was present underneath this soft compressible layer. The exact total thickness of this natural soil was not indicated in the geotechnical study but was expected to be about 100 feet, based on available geological information. At the time of the geotechnical investigation, groundwater was present at a depth of about 10 feet. The ground water level is tidally influenced and at certain times of the year, the groundwater level was just below the ground surface.

Design of CMC System

Settlements and stresses in the CMCs were computed using the FEM software Plaxis and an axisymmetrical model of the unit cell composed of the CMC and its surrounding soils. Soils and CMC properties used in the computations are summarized in Table 1.

TABLE 1 Characteristics of the Soil Layers Used in the FEM Analysis

Material	Thickness (ft)	Young's modulus (psf)
Upper sandy fill	16	375,900
Organic silt	8	62,660
Lower dense sand	±100	626,600
Load transfer platform	2	1,044,000
CMC	26	365,500,000

Computation results are summarized in Table 2 below.

TABLE 2 Results of FEM Analysis for the Unit Cell

Grid spacing (ft x ft)	Column diameter (inches)	Settle-ment (inches)	Column stress (psi)
5 x 5	12	3.4	750

Modeling Of Tank Using Equivalent Soil Modulus

In order to estimate the differential settlement due to the tank geometry itself, an axisymmetrical model of the whole tank and the improved soil was used. The modulus of the improved composite soils used in the calculations is an equivalent modulus computed from the results of the axisymetrical unit column model.

The equivalent Young's modulus of the composite soil is based on the computed settlement and the stress (σ) applied on top of the CMCs per the following elastic relationship:

$$\frac{\Delta H}{H} = \frac{\sigma}{E_{equivalent}}$$

Where ΔH is the settlement and H is the total thickness of the composite layer, CMC and the load transfer platform. Based on the calculated results for the unit cell model, the equivalent modulus of the reinforced soil mass was estimated at 584,800 psf. The load applied by the tank was 5,000 psf. All other soil parameters were kept similar to the previous model.

The axisymmetrical calculation results are shown graphically on Figure 4. Based on this model, the settlement at the center of the tank was expected to be approximately 3.15 inches, and the settlement under the ring wall was about 2 inches with a differential settlement between the center and the edge of approximately 1.1 inch as shown on Figure 4.

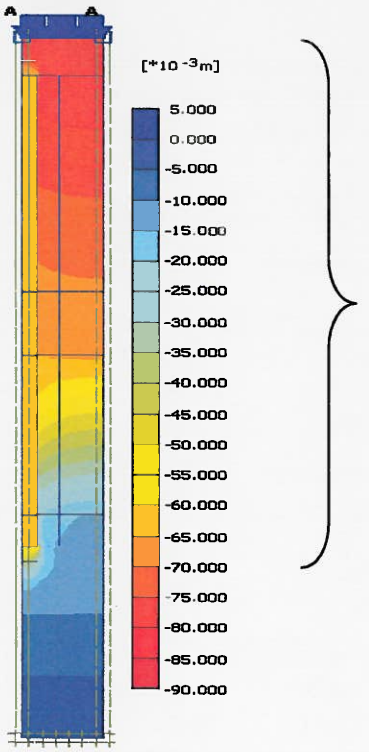

FIGURE 4 FEM settlement computation results for the unit cell.

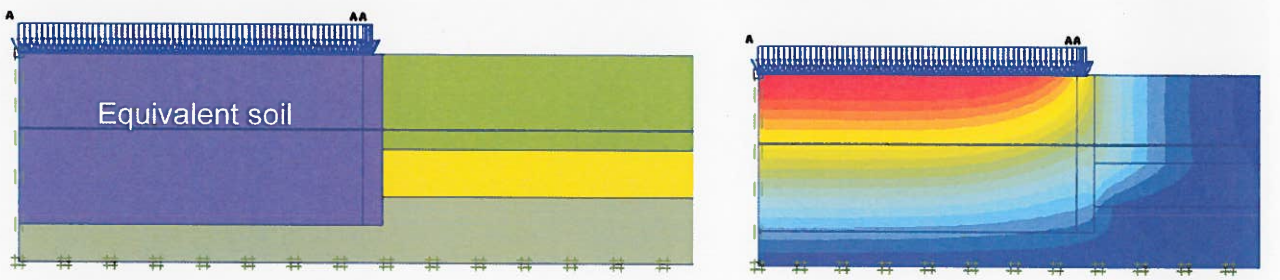

FIGURE 5 Model and results of FEM computations of the soils under the tank load.

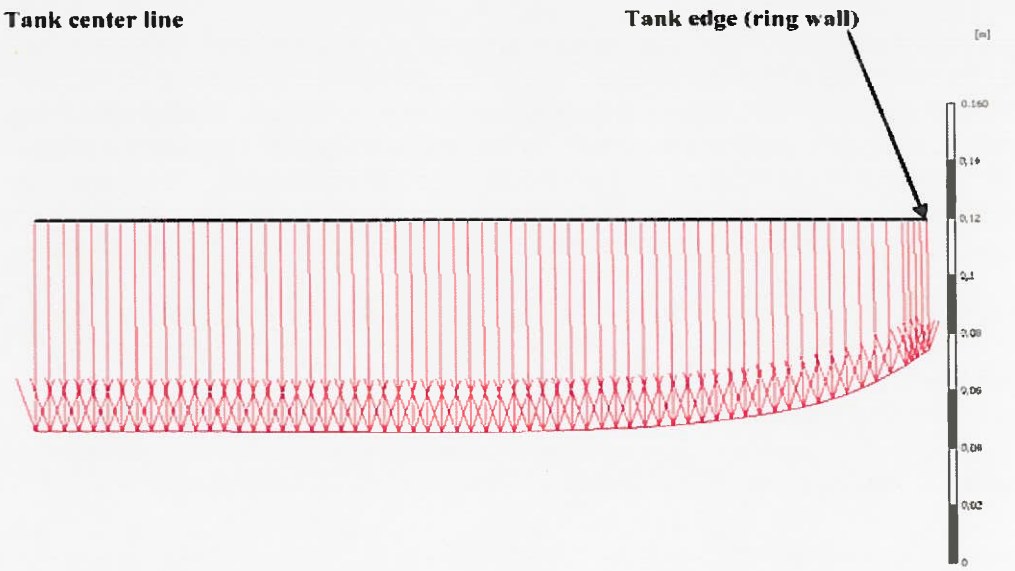

FIGURE 6 Predicted settlements under the tank load.

The calculated differential settlement results are on the conservative side since the previous model did not take into consideration the following factors:

- the depth of embedment of the tank
- the increased rigidity of the outer edge (ring wall) of the tank

On this basis, it was considered that the differential settlement between the ring wall and the center of the tank would be less than 1 inch.

Construction and Measured Settlements

During the tank hydro-test water test, settlements varying between 1 and 1.4 inches were measured along the periphery of the tanks. These values, smaller than those computed, can be explained by the use of conservative material properties and by the fact that the effect of soil densification between the inclusions was ignored in the models. Nevertheless, it shows that relatively accurate settlement estimations, with a conservative safety margin, can be obtained with the methods describe herein.

FIGURE 7 Installation of the CMCs in Quebec City.

CASE HISTORY – TEXAS CITY, TX

In Texas City, Texas CMCs were used to support a total of seven new tanks at an existing oil refinery tank farm. One tank was 62 feet in diameter, four of the tanks were 115 feet in diameter, and two tanks were 150 feet in diameter. The product heights for the tanks were 56 feet. In addition to supporting the storage tanks, CMCs were also used to support earthen ramps which were constructed to allow access into the tank area, which was encircled by reinforced concrete containment walls. The ramps were constructed to provide a convenient and safe access for equipment and vehicles to enter the storage tank area.

The site is underlain by a layer of clayey fill that varies in thickness across the site. Below this layer lies a soft to medium stiff clay, which increases in stiffness extending to a depth of 40 feet. A layer of stiff to hard clay is present below the softer clay layer. Without ground improvement, significant settlement would have occurred for both the tanks and the access ramps.

Design of the CMC System

The design was performed using a 2D axisymetrical model in Plaxis. The settlement of the deeper layers below the tip of the CMCs was evaluated using classical consolidation theory by hand. To estimate the total long term settlement of the system, both settlement estimations were added together.

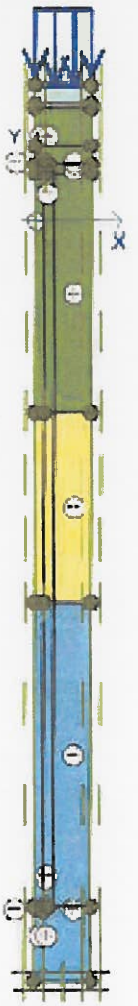

ID	Name	Type	γ_{unsat} [lb/ft^3]	γ_{sat} [lb/ft^3]	k_x [ft/day]	k_y [ft/day]	E_{50}^{ref} [lb/ft^2]	E_{oed}^{ref} [lb/ft^2]	E_{ur}^{ref} [lb/ft^2]
1	Stiff Clay	Drained	125.0	125.0	283.0000	283.0000	30475.0	30475.0	2.435E5
2	Medium Clay	Drained	125.0	125.0	283.0000	283.0000	27089.0	27089.0	2.191E5
3	Granular Fill	Drained	125.0	125.0	283.0000	283.0000	1.9845E6	1.9845E6	5.9535E6
4	Fill	Drained	120.0	120.0	283.0000	283.0000	27089.0	27089.0	2.191E5
6	Bedding Sand	Drained	120.0	120.0	283.0000	283.0000	5.292E5	5.292E5	1.5876E6
7	Clay Liner	Drained	125.0	125.0	283.0000	283.0000	2.705E5	2.705E5	1.353E6

FIGURE 8 Model properties – Axisymmetrical Model.

The model is shown above. A soil-Hardening behavior law was selected for all layers except the CMC itself which was defined an elasto-plastic material.

FIGURE 9 Deformed mesh plaxis.

FIGURE 10 Vertical displacement plaxis.

The calculated settlements are summarized below in Table 3. Two types of analysis (best and worst case) were performed. Estimated total settlements ranged from 7.8 inches to 10.3 inches.

TABLE 3 Estimated Settlements in Best and Worst Case

Zone of Settlement	Settlement, inches	
	Least	Greatest
Within CMC – Reinforced Zone	Directly Above CMC	Between CMC's
	4.500	4.632
Below CMC – Reinforced Zone	Edge of Tank	Center of Tank
	3.29	5.69
Total	Minimum	Maximum
	7.79	10.32
Differential	2.53	

Two single element load tests were installed in order to verify the assumptions of the design. Based on the results of the FEM analysis, the design load was 115 kips. At design load, the movement of the CMCs was under a quarter of an inch which was well within the design parameters.

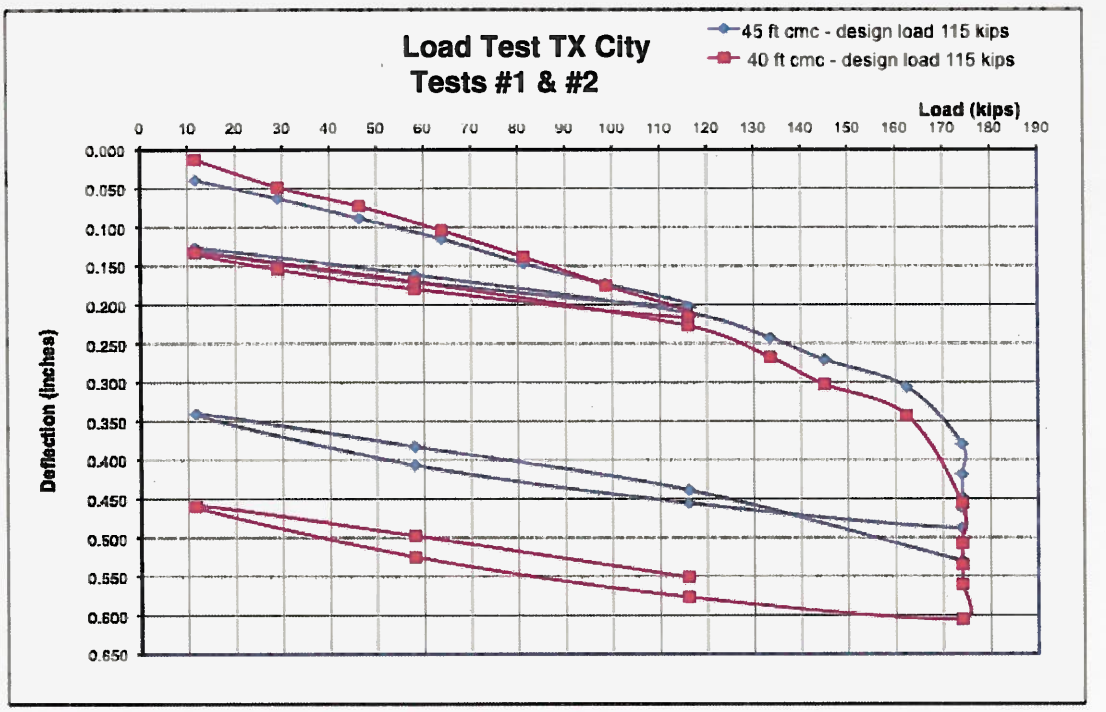

FIGURE 11 Plot of two load tests performed on a 40 ft and a 45 ft CMC.

The CMC ground improvement solution consisted of the installation of a total of 1,800 CMCs, to maximum depths of 45 feet. Over 77,000 lf of CMCs, 12.5-inches in diameter were installed.

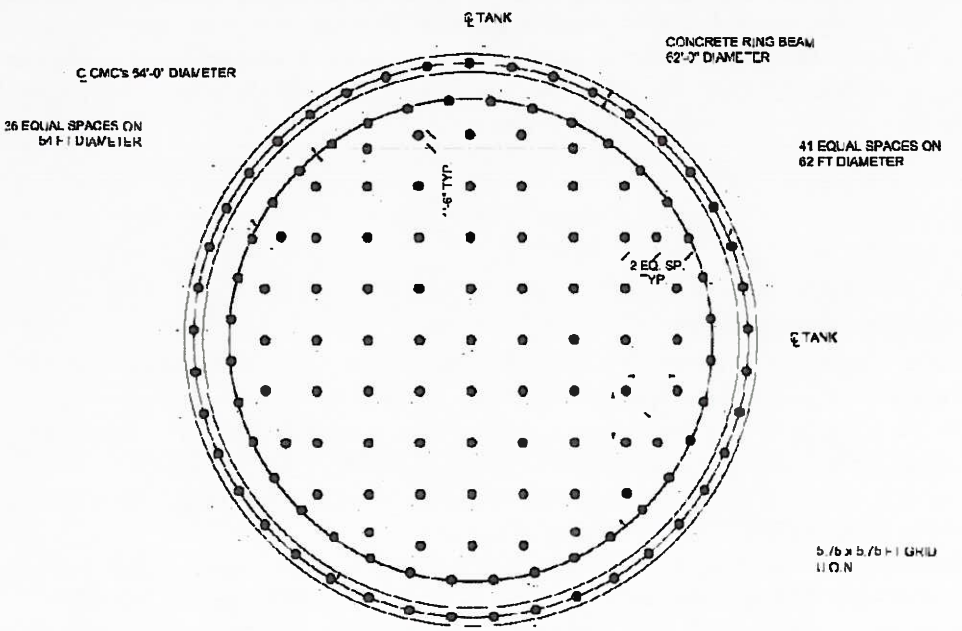

FIGURE 12 Typical layout under 62 ft diameter tank.

FIGURE 13 Texas City CMC installation site.

CONCLUSION

CMC technology spans a wide range of economical solutions for heavily loaded structures when piling or other deep foundations are the initial means for gaining support. By eliminating heavy structural mats and pile caps, while at the same time allowing the compatible sharing of support with the soil, results in the optimal use of all materials. Since the elements do not drain, long term consolidation is discouraged, and undesirable vertical transport of groundwater contaminants is not promoted. Spoil generation is nil, eliminating the costly disposal of contaminated ground. Performance is more predictable and subject to less variation, since real time monitoring allows for adjustment of column depth as the site is traversed and the bearing conditions vary. Speed of construction is enhanced since traditional steps (like surcharging and concrete construction) are eliminated.

REFERENCES

1. F. Masse, Pearlman, P.E., Bloomfield, P.E. - Support of MSE walls and reinforced embankments using ground improvement
2. Collin, J.G. & al (2004) – FHWA - NHI Ground improvement manual – Technical summary #10: Columns supported embankment – FHWA – 2004
3. Dumas, C. & al (2003) Innovative technology for accelerated construction of bridge and embankment foundations in Europe - FHWA-PL-03-014, FHWA 2003
4. Masse, F. & al. (2004) CMC: potential application to Canadian soils with a new trend in ground improvement - CGS 2004, Winnipeg, Canada
5. Plomteux, C. Spaulding, C., Simmons, G. (2003) – "*Reinforcement of Soft Soils by Means of Controlled Modulus Columns*"– *Soil and Rock America* 2003, pp 1687-1694
6. Plomteux, C. & al (2003) – "*Controlled Modulus Columns (CMC): Foundation system for Embankment support: a case history*" – *Geosupport 2004,* Orlando, USA, pp 980-992
7. Porbaha, A. & al (2007) – *"Design and monitoring of an embankment on controlled modulus columns" TRB paper #06-1743 – Transportation Research Board*, 2007

8. Plaxis finite element code for soil and rock analysis user's manual – Plaxis V8 – 2007
9. LACZAEDIEU, M., PLOMTEUX, C., CORBET, S., SHAW-SMITH, E. - Intensive Ground Improvement using CMC for the Newport Southern Distributor Road (Wales) – FABER MAUNSELL Ltd, Enterprise House, 160 Croydon Road, Beckenham, BR34DE, UK
10. Plomteux, C., Porbaha, A. (2004) CMC Foundation System for Embankment Support-A Case History-ASCE conference 2004
11. Berthelot, P., Pezot, B., Liausu, Ph. – Amelioration des sols naturels ou anthropiques par colonnes semi-rigides: Le procede CMC – XIIIth European Conference on Soil Mechanics and Geotechnical Engineering (ECSMGE) – Praha, Czech Republic – August 2003
12. Liausu, Ph., Pezot, B. – Reinforcement of soft soils by means of controlled modulus columns – XVth International Conference of Soil Mechanics and Geotechnical Engineering (ICSMGE) – Instanbul, Turkey-September 2001
13. Rogbeck, Y. (1998)-Two and Three dimensional numerical analysis of the performance of piled embankment-6th International Conference on Geosynthetics, Atlanta
14. Rogbeck, Y., Gustavson, S., Sodergren I., Lindquist D. (1998) – Reinforced piled embankments in Sweden-Design Aspects-6th International Conference of Geosynthetics, Atlanta
15. Combarieu, O. (1988) – Amelioration des sols par inclusions rigides verticals – application a l'edification de remblais sur sols mediocres-Revue Francaise de geotechnique n 44, pp. 57-59
16. Combarieu, O. (1988)-Calcul d'une foundation mixte-Note d'information technique LCPC
17. Plomteux, C. and Porbaha, A. - CMC Foundation System for Embankment Support - - A Case History
18. Porbaha, A., Brown, D., Macnab, A., Short, R. (2002a) *Innovative European technologies to accelerate construction of embankment foundations- part 1: GEC, AuGeo, and CFA. Proceedings of Time Factor in Design and Construction of Deep Foundations*, Deep Foundation Institute, San Diego, CA, October, 3-14
19. Porbaha, A., Brown, D., Macnab, A., Short, R. (2002b) *Innovative European technologies to accelerate construction of embankment foundations- part II: DM, FMI, Mass Stabilization, and CSV. Proceedings of Time Factor in Design and Construction of Deep Foundations*, Deep Foundation Institute, San Diego, CA, October, 15-28.
20. Rogbeck, Y. & al. (1998) *"Two and three dimensional numberical analysis of the performance of piled embankment"* 6th International Conference on Geosynthetics, Atlanta
21. Rogbeck, Y. & al. (1998) *"Reinforced piled embankments in Sweden – Design Aspects:* 6th International Conference on Geosynthetics, Atlanta
22. Sanglerat, G. (199?) The Penetrometer and soil exploration Interpretation of penetration diagrams – theory and practice, Part 3 – Page 285

EVALUATION OF KARSTIC FOUNDATION HAZARDS FOR NEW POWER PLANT CONSTRUCTION AT A SITE IN CENTRAL FLORIDA

Barry F. Beck, Arthur Pettit, and Wanfang Zhou[1]
P.E. LaMoreaux & Associates, Inc.
160 Bus Terminal Road, Ridgeway Center #160
Oak Ridge, Tennessee

The Orlando, Florida, area is a mantled karst terrane: that is, the limestone is overlain by younger, unconsolidated sediments. The power plant site under discussion is located generally southwest of Orlando. It is a slightly elevated sandy area, approximately one mile long and 1,000 feet wide, surrounded by swamps.

Beneath the Orlando area, the Ocala Group limestones of Eocene age are overlain by clayey sediments of Miocene age, the Hawthorn Group, and more recent sands and clay at the surface. The total thickness of unconsolidated clays and sands over the limestone varies from zero to 200 feet. At the power plant site the depth to limestone is approximately 70 feet, except in areas of greater karstic dissolution. The Ocala limestone is the uppermost in a thick sequence of limestones which are riddled with dissolved cavities: the highly permeable Floridan Aquifer. Water in this aquifer is confined by the clays above the limestone. An unconfined aquifer in the surficial sands is perched above the clay. The surface water table is generally higher than the artesian pressure (potentiometric level) of the Floridan Aquifer, driving recharge downward through the clay. It is this downward movement of water which erodes the clay downward into the dissolved cavities in the limestone causing sinkholes.

Sinkholes are characteristic of a karst terrane, a type of landscape formed on soluble rock, most frequently limestone. In a karst terrane drainage is internal: downward into the limestone through dissolved channels. If unconsolidated sediments overlay the limestone, these may be eroded downward through these channels resulting in depressions in the land surface. If the near surface sediments are cohesive they may remain unaltered while erosion proceeds upward from below. Eventually the surface will either collapse suddenly (Figure 2) or gradually "sag" downward due to the lack of support from below (Figure 3).

The subsurface zone which is being undermined by karstic erosion is called a "ravelling" zone by engineers. It is characterized by very low bearing strength sediments: in the SPT test, 0 to 1 or 2 blows per foot. Because these are located over channels where the limestone has been intensely dissolved, the depth to limestone is greater. Obviously such ravelling zones are foundation hazards, particularly for heavy loads. The downward erosion process is continuous over time, although it may be sporadic in the short term. Downward erosion may be ongoing at depth, but its effect may not have reached the

[1] At the time of the project work Wanfang Zhou was a member of the PELA staff.

ground surface. The presence of a ravelling zone at depth indicates that karstic erosion is occurring.

The landforms (geomorphology) of the Orlando area are also related to areas of sinkhole occurrence. The western portion of the metropolitan area is located on three high, sandy ridges, whereas the eastern part is generally low, swampy ground. Recharge rates are highest beneath the three ridges and lower in the swampy plain. Most sinkholes also develop on the ridges.

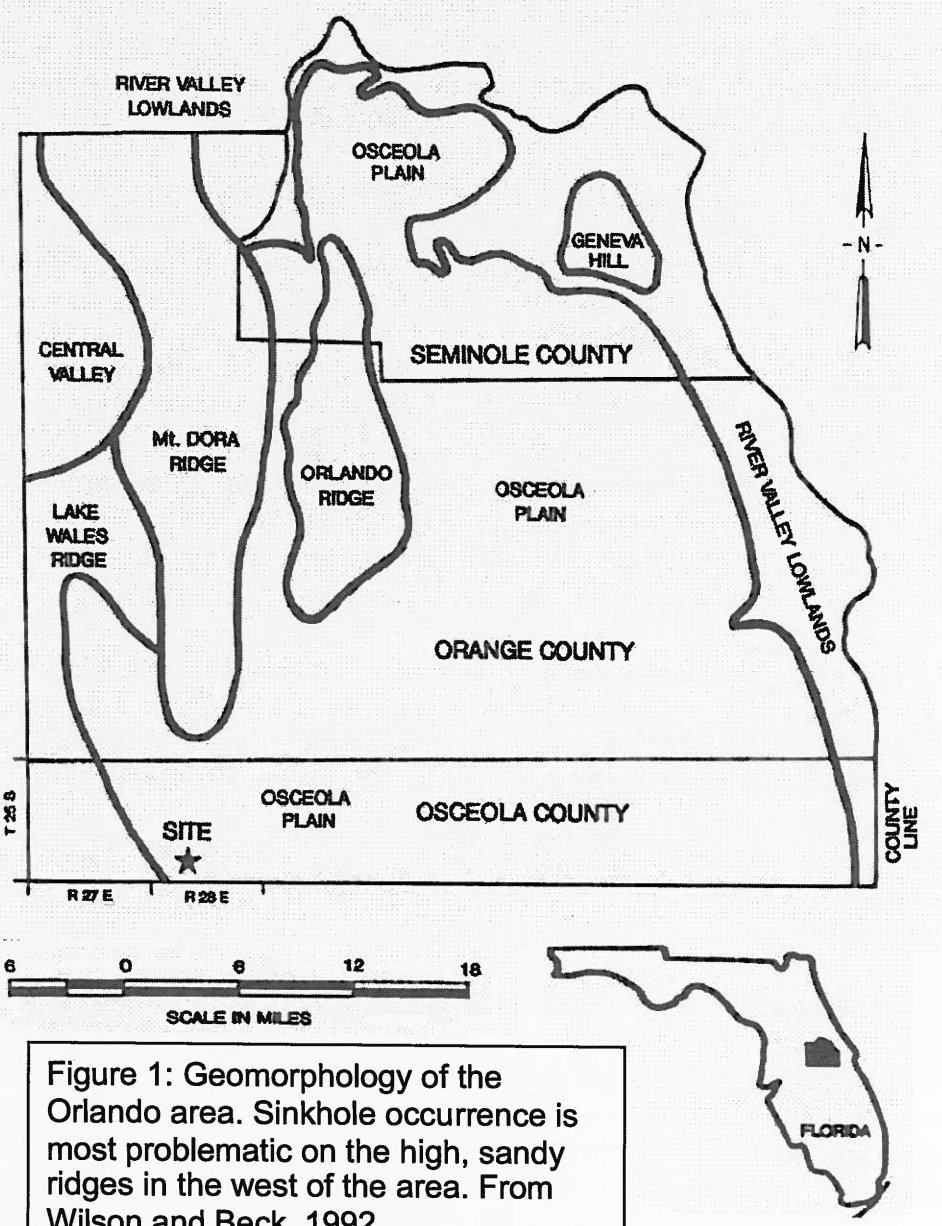

Figure 1: Geomorphology of the Orlando area. Sinkhole occurrence is most problematic on the high, sandy ridges in the west of the area. From Wilson and Beck, 1992.

The power plant site is similar to the ridges, although on a much smaller scale. The water table beneath the elevated sandy area is higher than beneath the surrounding swamp, causing downward recharge which is the driving force for karstic erosion. Data compiled by the Florida Sinkhole Research Institute indicates that the risk of sudden sinkhole collapse is very low at the site. Sinkhole collapses are not common here because the head difference is minimal due to the low elevation of the site. However, the potential hazard from karstic erosion is still present. Slow, gradual subsidence may occur over these zones, particularly under heavy foundation loads. Structures only partially over a buried sinkhole may experience differential settlement.

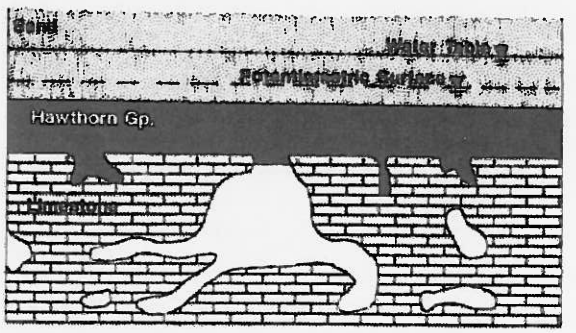

Fig. 5a. Generalized sketch of hydrogeologic conditions in the Orlando area. The limestone is riddled with irregular dissolution voids, which are generally plugged by clayey Hawthorn Gp. sediments along the contact. Ground water in the surface sands is perched on the Hawthorn, and ground water in the limestone is confined by it.

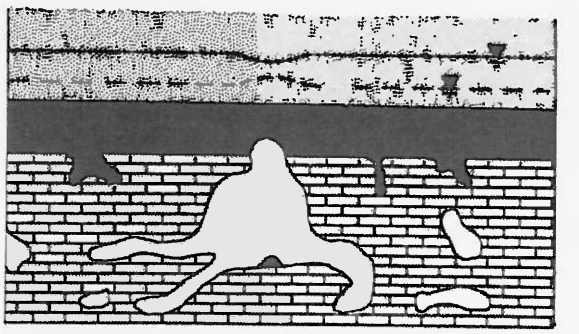

Fig. 5b. Conceptual model of the onset of sinkhole collapse. The sediment plugging a dissolution cavity begins to erode downward. Details of the mechanism are unknown. Downward leakage of ground water is greater here and a cone-of-depression forms in the surficial water table while a recharge mound results in the "confined" aquifer.

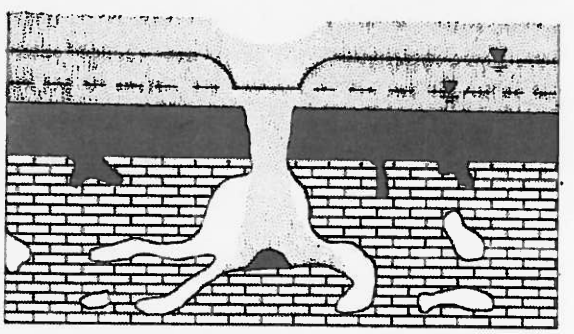

Fig. 5c. The durable confining layer is completely breached by stoping collapse and the overlying loose sand rapidly subsides. The water level in the actively collapsing sinkhole may even be pulled below the potentiometric surface by the density of the subsiding sediment.

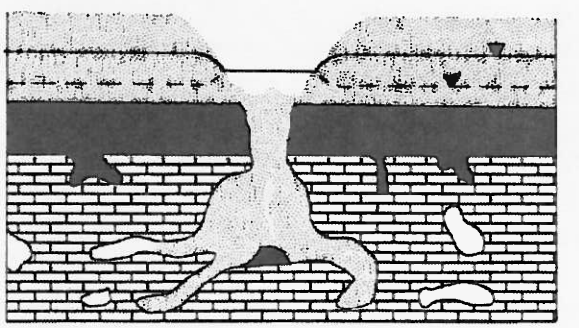

Fig. 5d. Active downward erosion ceases. In most cases the breach through the confining layer is filled with permeable collapsed sediment. The sides of the sinkhole will gradually erode to a stable slope angle. The water level in the hole is a balance between inflow from the sand and leakage through the permeable plug.

Figure 2: Schematic diagram of the development of a cover-collapse sinkhole in the Orlando area (from Wilson and Beck, 1992).

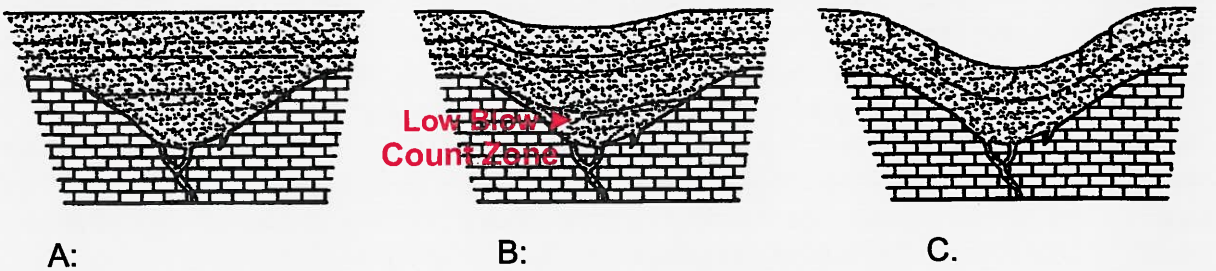

Figure 3: Formation of a cover-subsidence sinkhole in the Central Florida area. Left to right: A: Solution sinkhole infilled and covered over with more recent sediments; B: Downward karstic erosion slowly undermines the sediment creating a low density zone (low blow count zone) over the karstic shaft; C: Overlying sediment slowly and gradually "sags" (possible plastic flow) over time. Rate = inches/year . (From: Beck, 2005.)

Data from exploratory drilling is not sufficient to document this hazard: The borings are too far apart. A continuous cross-section, such as can be made with GPR, is highly cost-effective. GPR emits a beam of radar waves downward into the ground and detects the reflections of these waves from various geologic features. The antenna is pulled across the ground surface, producing a continuous cross-section. Because GPR generally performs well in sandy areas, it has been applied here.

In the 1993 investigation GPR profiles over the anomalous borings demonstrated clearly that these were areas of deep karstic erosion and that such features were more extensive than interpretation of the standard penetration test (SPT) results had indicated. The data from the profiles were compiled onto a large-scale map of the site delineating areas where ravelling zones were probably present. The original foundation borings and supplementary data all corroborated the GPR findings on the map. Uncontrolled GPR profiles to the north of the site indicated that a similar problem should be anticipated there.

For the construction of additional power plant facilities to the north of the previous construction, PELA was engaged in 2007 to conduct a karst hazard investigation of the site expansion. The core of the investigation was to be an extension of the earlier GPR grid of the site, but the new phase was also to include natural electrical potential (NP) measurements over possible areas of subsidence indicated on the radar graphs. NP responds to the downward leakage of water and is used to indicate recharge areas which are most at risk for future collapse or subsidence. SPT borings were also made in the larger areas of potential subsidence and in nearby, undisturbed locations. This investigation was to evaluate the karstic hazards beneath the expanded site and was not intended as a geotechnical evaluation.

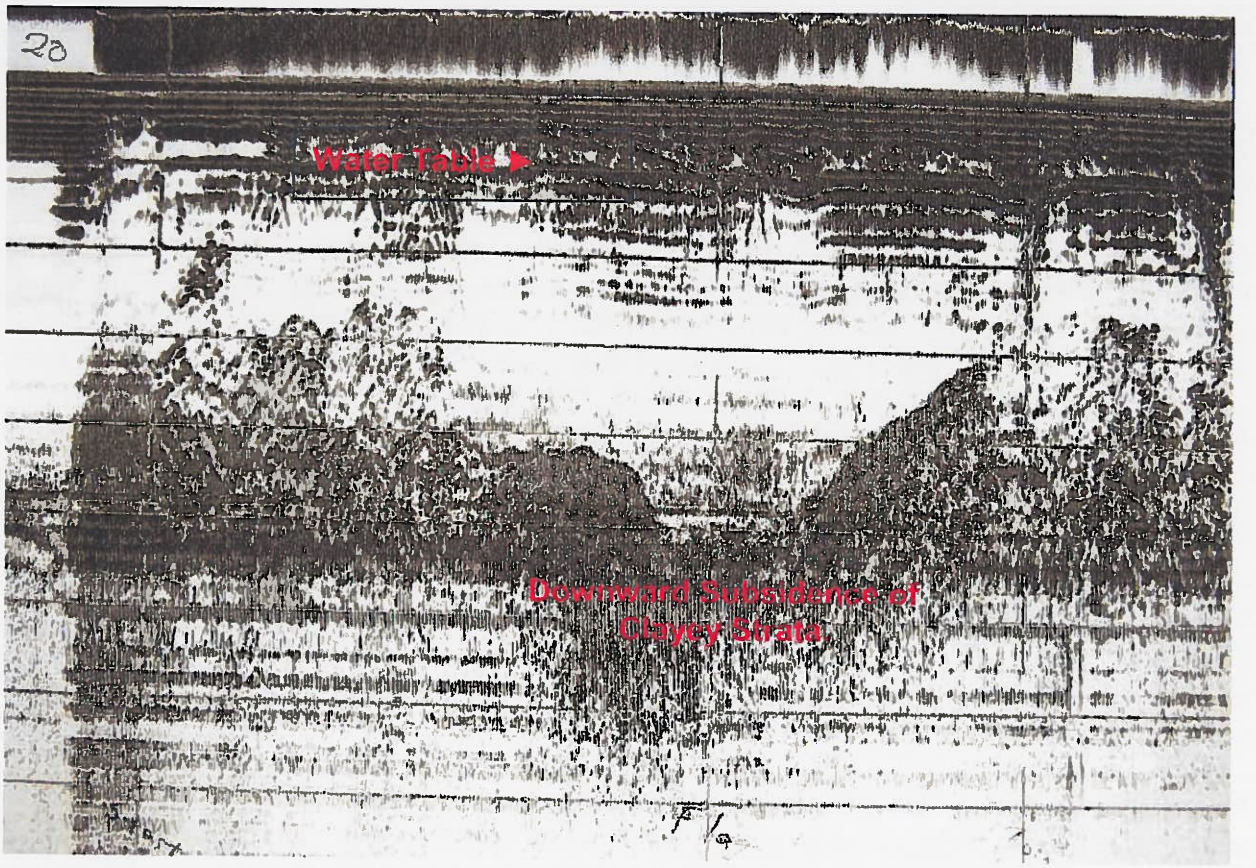

Figure 4: Sample GPR record showing subsidence. The interface demonstrating the subsidence is within the sandy overburden sediment. The limestone hosting the karst is approximately 70 feet below the land surface. Note also that the water table is irregular above the subsidence indicating that there may be downward leakage occurring.

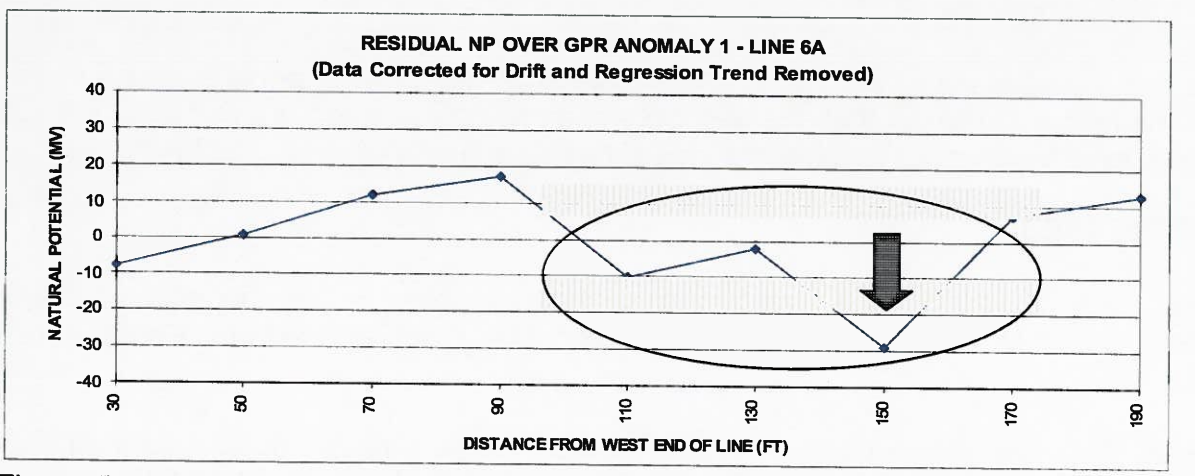

Figure 5: Natural electrical potential transect across the site. The distinct low in the NP readings may indicate downward leakage at that location.

Five significant areas and numerous smaller or less definite areas of karstic undermining were detected on the new site by GPR. The NP data indicated several areas where downward leakage was probable and several areas where such leakage was possible, but less definite. Moreover, water level data from the SPT borings confirmed one area of downward leakage.

The 1993 report did not include NP measurements or analysis of water levels. Therefore, it is unknown whether similar areas of leakage existed on the original site. Given the continuity and similarity of the areas, it is quite probable that similar leakage zones were present there and simply went undetected. The buried areas of karstic erosion shown on the map are significant long-term foundation hazards for heavy structures. *However, conditions in the expanded area do not appear to be significantly different from what was mapped and remediated for the earlier construction.* That remediation has been successful to date.

As part of the geotechnical investigation of the site, SPT borings were also made to bedrock to investigate the various potentially hazardous areas identified by GPR. Selected borings were converted to piezometers when completed. Nested deep and shallow piezometers will provide the most information and were installed in the areas of potential karstic activity.

The original investigation did not consider the impact of ground water withdrawal in the site vicinity. Several deep water supply wells are located in the site vicinity and several additional wells are planned for the future use of the power plant. Drawdown of the deep potentiometric surface could increase the shallow/deep head difference and has been documented to trigger sinkhole collapse in other settings. However, modeling of the site conditions and pumping tests indicate very limited areas of significant drawdown immediately around the wells such that this should not create an increased risk for appropriately planned development. To avoid exacerbating the shallow/deep head difference, surface water drainage facilities (retention basins) should not be located over any of the karst features.

The final conclusions of the site analysis, based on geophysics, borings, pump testing, and modeling, indicated that the site development could be expanded, as planned in view of the karst testing, and that the risk of karstic subsidence would be low.

REFERENCES

Beck, Barry F., 2005, Soil piping and sinkhole failures: *in* Encyclopedia of Caves, Culver, D.C. and White, W.B. (ed's), Burlington, MA, Elsevier Academic Press, p. 521-526.

Wilson, W.L. and Beck, Barry F., 1992, Hydrogeologic factors affecting new sinkhole development in the Orlando area, Florida: Ground Water, V 30, n 6, p 918-930.

PAST OHIO RIVER VALLEY SOILS SEMINARS

ORVSS I	BUILDING FOUNDATION DESIGN AND CONSTRUCTION, October 16, 1970, Lexington, KY.
ORVSS II	EARTHWORK ENGINEERING, START TO FINISH, October 15, 1971, Louisville, KY.
ORVSS III	LATERAL EARTH PRESSURES, October 27, 1972, Fort Mitchell, KY.
ORVSS IV	GEOTECHNICS IN TRANSPORTATION ENGINEERING, October 5, 1973, Lexington, KY.
ORVSS V	ROCK ENGINEERING, October 18, 1974, Clarksville, IN.
ORVSS VI	SLOPE STABILITY AND LANDSLIDES, October 17, 1795, Fort Mitchell, KY.
ORVSS VII	SHALE AND MINE WASTES: GEOTECHNICAL PROPERTIES, DESIGN, AND CONSTRUCTION, October 8, 1976, Lexington, KY.
ORVSS VIII	EARTH DAMS AND EMBANKMENTS: DESIGN, CONSTRUCTION AND PERFORMANCE, October 14, 1977, Louisville, KY.
ORVSS XIV	DEEP FOUNDATIONS, October 27, 1978, Fort Mitchell, KY.
ORVSS X	GEOTECHNICS OF MINING, October 5, 1979, Lexington, KY.
ORVSS XI	EARTH PRESSURE AND RETAINING STRUCTURES, October 10, 1980, Clarksville, IN.
ORVSS XII	GROUNDWATER: MONITORING, EVALUATION AND CONTROL, October 9, 1981, Fort Mitchell, KY.
ORVSS XIII	RECENT ADVANCES IN GEOTECHNICAL ENGINEERING PRACTICE, October 8, 1982, Lexington, KY.
ORVSS XIV	FOUNDATION INSTRUMENTATION AND GEOPHYSICAL EXPLORATION, October 14, 1983, Clarksville, IN.
ORVSS XV	PRACTICAL APPLICATION OF DRAINAGE IN GEOTECHNICAL ENGINEERING, November 2, 1984, Fort Mitchell, KY.
ORVSS XVI	APPLIED SOIL DYNAMICS, October 11, 1985, Lexington, KY.
ORVSS XVII	NATURAL SLOPE STABILITY AND INSTRUMENTATION, October 17, 1986, Clarksville, IN.
OVRSS XVIII	LIABILITY ISSUES IN GEOTECHNICAL ENGINEERING AND CONSTRUCTION, November 6, 1987, Fort Mitchell, KY.
ORVSS XIX	CHEMICAL AND MECHANICAL STABLIZATION OF SOIL SUBGRADES, October 21, 1988, Lexington, KY.
ORVSS XX	CONSTRUCTION IN AND ON ROCK, October 27, 1989, Louisville, KY.
ORVSS XXI	ENVIRONMENTAL ASPECTS OF GEOTECHNICAL ENGINEERING, October 26, 1990, Fort Mitchell, KY.

PAST OHIO RIVER VALLEY SOILS SEMINARS (CONT.)

ORVSS XXII	DESIGN AND CONSTRUCTION WITH SYNTHETICS, October 18, 1991, Lexington, KY.
ORVSS XXIII	IN-SITU SOIL MODIFICATION, October 16, 1992, Louisville, KY.
ORVSS XXIV	GEOTECHNICAL ASPECTS OF INFRASTUCTURE RECONSTRUCTION, October 15, 1993, Fort Mitchell, KY.
ORVSS XXV	RECENT ADVANCES IN DEEP FOUNDATIONS, October 21, 1994, Lexington, KY.
ORVSS XXVI	SITE INVESTIGATIONS: GEOTECHNICAL AND ENVIRONMENTAL, October 20, 1995, Clarksville, IN.
ORVSS XXVII	FORENSIC STUDIES IN GEOTECHNICAL ENGINEERING, October 11, 1996, Cincinnati, OH.
ORVSS XXVIII	UNCONVENTIONAL FILLS: DESIGN, CONSTRUCTION AND PERFORMANCE, October 10, 1997, Lexington, KY.
ORVSS XXIX	PROBLEMATIC GEOTECHNICAL MATERIALS, October 16, 1998, Louisville, KY.
ORVSS XXX	VALUE ENGINEERING IN GEOTECHNICAL CONSULTING AND CONSTRUCTION, October 1, 1999, Cincinnati, OH.
ORVSS XXXI	INSTRUMENTATION, September 15, 2000, Lexington, KY.
ORVSS XXXII	REGIONAL SEISMICITY AND GROUND VIBRATIONS, October 24, 2001, Louisville, KY.
ORVSS XXXIII	GROUND STABILIZATION AND MODIFICATION, October 18, 2002, Covington, KY.
ORVSS XXXIV	APPLICATIONS OF EARTH RETAINING SYSTEMS AND GEOSYNTHETIC MATERIALS, September 19, 2003, Lexington, KY.
ORVSS XXXV	ROCK ENGINEERING AND TUNNELING, October 20, 2004. Louisville, KY.
ORVSS XXXVI	GEOTECHNICAL INNOVATIONS IN TRANSPORTATION ENGINEERING, October 14, 2005, Covington, KY.
ORVSS XXXVII	INNOVATIONS IN EXPORATION OF SUBSURFACE VOIDS, October 27, 2006, Lexington, KY.
ORVSS XXXVIII	CIVIL INFRASTRUCTURE AND THE ROLE OF GEOTECHNICAL ENGINEERING, November 14, 2007, Louisville, KY.
ORVSS XXXIX	URBAN CONSTRUCTION, October 17, 2008, Covington, KY.
ORVSS XL	GEOTECHNICAL ENGINEERING and ENERGY INFASTRUCTURE, November 13, 2009, Lexington, KY.